

1973

Deformation and structural changes occurring at the interface during gold-gold thermocompression bonding

Leon Dries
Lehigh University

Follow this and additional works at: <https://preserve.lehigh.edu/etd>



Part of the [Materials Science and Engineering Commons](#)

Recommended Citation

Dries, Leon, "Deformation and structural changes occurring at the interface during gold-gold thermocompression bonding" (1973).
Theses and Dissertations. 4205.
<https://preserve.lehigh.edu/etd/4205>

This Thesis is brought to you for free and open access by Lehigh Preserve. It has been accepted for inclusion in Theses and Dissertations by an authorized administrator of Lehigh Preserve. For more information, please contact preserve@lehigh.edu.

4

19

DEFORMATION AND STRUCTURAL CHANGES OCCURRING
AT THE INTERFACE DURING
GOLD-GOLD THERMOCOMPRESSION BONDING

by

Leon Dries

A Thesis

Presented to the Graduate Committee

of Lehigh University

in Candidacy for the Degree of

Master of Science

in

Metallurgy and Materials Science

Lehigh University

1973

CERTIFICATE OF APPROVAL

This thesis is accepted and approved in partial fulfillment
of the requirements for the degree of Master of Science.

April 16, 1973
Date

Alan W. Penee
Professor in Charge

G. P. Conrad
Chairman of the Department
of Metallurgy and Materials Science

Acknowledgements

The author wishes to thank Dr. J. J. Svitak for his helpful direction throughout the course of this work. Not only did he provide the kernel idea for this investigation, but he also provided technical information and inspiration along the way.

Appreciation is also extended to Dr. A. W. Pense for his support and useful suggestions during the course of this work.

The author also acknowledges the contributions of the members of Department 02225 of Western Electric's Engineering Research Center. Their assistance and advice saved many hours in the initialization and performance of the experiments.

The author thanks Western Electric Company and the Engineering Research Center for providing the facilities to carry out this investigation.

Table of Contents

	<u>Page</u>
Abstract	1
I. Introduction	3
II. Experimental Procedure	8
III. Results and Discussion	14
IV. Summary and Conclusions	28
Bibliography	58
Appendices	
A - Gold Plating for Substrate Generation	60
B - Marker Generation	62
C - Silver Plating Solution and Procedures	65
D - A Pure Gold Polishing Technique	67
Vita	69

List of Tables

	<u>Page</u>
Table 1 - Tape and Plated Substrate Metallization Parameters.	30
Table 2 - Hardness Values of Annealed Gold.	31

List of Figures

	<u>Page</u>
Fig. 1 - Substrate Plating Fixture.	32
Fig. 2 - As-Received Microstructure of Gold Ribbon.	33
Fig. 3 - VDPH Measurements as a Function of Annealing Temperature.	34
Fig. 4 - Microstructure of Annealed Gold Ribbon.	35
Fig. 5 - Schematic Drawing of Silver Markers in a Gold Tape.	36
Fig. 6 - Typical Fast Rise and Fall Times for the Modified Keller Lab Bonder.	37
Fig. 7 - Thermode and Heater Cartridge Configuration.	38
Fig. 8 - Typical Force and Height vs. Time Oscillograph.	39
Fig. 9 - Photomicrograph of Sectioned Tape Showing Silver Markers and Reference Mask Overlay.	40
Fig. 10 - Microstructure of Quenched Tape and Plated Substrate Metallization.	40
Fig. 11 - Microstructure of Air-cooled Tape and Plated Substrate Metallization.	40
Fig. 12 - Marker Motion vs. Distance from the Center for 573°K (300°C).	41
Fig. 13 - Marker Motion vs. Distance from the Center for 643°K (370°C).	42
Fig. 14 - Normalized Marker Motion vs. $p_i/(p+h)_i$ Ratios.	43

List of Figures, Cont'd	Page
Fig. 15 - Normalized Marker Motion vs. Distance from Center.	44
Fig. 16 - Tape Surface Strains vs. Distance from Center.	45
Fig. 17 - Schematic Drawing Illustrating Definition of Surface Sliding, δ_s .	46
Fig. 18 - Photomicrograph of Interface Showing Proposed ΔL_p and δ_s .	47
Fig. 19 - Photomicrograph of Interface Showing Proposed ΔL_p and δ_s .	47
Fig. 20 - Normalized Surface Motion of Substrate Plating vs. Distance from Center.	48
Fig. 21 - Substrate Plating Strains vs. Distance from Center.	49
Fig. 22 - Scanning Electron Photomicrograph of Grain Boundary Swept Bond Interface.	50
Fig. 23 - Scanning Electron Photomicrograph Showing a Twin Crossing the Interface.	51
Fig. 24 - Scanning Electron Photomicrograph of Fig. 23 at Higher Magnification.	52
Fig. 25 - Reconstructed Reduction in Height vs. Time Curve.	53
Fig. 26 - Reduction in Height vs. Time Curves for Samples Deformed at 573°K (300°C).	54
Fig. 27 - Instantaneous Flow Stress, σ_o , for Specimens Deformed at 573°K (300°C).	55
Fig. 28 - Reduction in Height vs. Time Curves for Samples Deformed at 643°K (370°C).	56
Fig. 29 - Instantaneous Flow Stress, σ_o , for Specimens Deformed at 643°K (370°C).	57

Abstract

Thermocompression bonding has been investigated by deforming .254mm X 1.575mm X 9.526mm tapes against a gold film plated on a rigid substrate. This results in plane strain deformation, but otherwise conditions are as used in industrial practice. Experiments were carried out at temperatures of 573°K (300°C) and 643°K (370°C) with a nominal 15% reduction in height. Silver markers, electrodeposited into grooves etched into the surface of the tape, allowed the amount of deformation occurring at the interface to be determined. The effect of changes in geometry was investigated by varying the thickness of the plated gold on the substrate from 1µm to 100µm. Analysis of the marker motion and metallographic examination of the integrity of the bond interface defined conditions at the interface that are sufficient for bond formation.

Bonding occurred throughout the regions where there was surface elongation except at the very edges, where normal stresses are low. Surface elongation, as indicated by the marker motion, was dependent on the amount of height reduction and on the relative thickness of the substrate plating, but did not depend on temperature. The nominal 15% reduction in height resulted in a 12% surface elongation in regions towards the edges of the tape that was independent of the relative thickness of the substrate plating.

Surface strains nearer to the center, on the other hand, depended strongly on the relative thickness of the substrate plating. When the substrate plating was thin compared to the total height of the specimen, there was negligible surface elongation in the central region of the bond interface and bond formation did not occur. When the substrate plating accounted for about one eighth of the total initial height of the specimen or more, surface elongation in the central region was 12% or more and bond formation always occurred.

Immediate quenching of the bonded specimens showed that gold does not completely recrystallize during bonding though grain boundaries occasionally migrate across the interface. Preferential etching of the interface was usually observed which appears to be due to voids distributed along most of the bonded interface.

I. INTRODUCTION

The use of gold rectangular bars (beam leads) to connect integrated circuit chips to a metallized substrate is a widely used method of fabricating electronic circuits. The beam lead can be electrically and mechanically connected to the metallized substrate by thermocompression bonding. To provide electrical continuity with external circuitry, gold plated rectangular bars of copper can be thermocompression bonded to the same substrate. The interface between the lead and the metallized substrate to be joined are brought to some elevated temperature, usually between 523°K - 823°K (250°C - 550°C), and enough force applied to deform at least one of the members¹. There have been optimization investigations of parameters and methods, for example, by Anderson, Christenson and Andreatch², McCann and Reid³, Clark⁴, Coucoulas⁵, Deutsch⁶, and Adams and Bonham⁷.

Anderson⁸ investigated the effect of tangential shear stresses that were induced by twisting, on the electrical conductivity and the seizure occurring between two gold balls. Deutsch⁶ and Ellington⁹ have indicated that deformation is important to the formation of thermocompression bonds between gold plated copper leads and gold metallized substrates. Some of the above investigators^{3,4,7} and the proposed SAE bonding standard¹⁰, have indicated that deformation is important to the formation of beam lead thermocompression bonds. These references consider the effect that overall

deformation of the pieces has on bond formation. There does not appear to be any studies of the deformation and structural changes occurring at the interface during the thermocompression bonding of gold to gold in the literature. However, since thermocompression bonding is just a specialized solid state joining process, investigations of the bonding of other metals and of other solid state bonding processes are pertinent.

Milner and Rowe¹¹ and Tylecote¹² have reviewed the principles of solid phase joining of metals and discuss evidence that indicates the importance of deformation. There are two modes of deformation occurring at an interface that may be of importance to bond formation. One is the amount of surface elongation or surface extension that occurs on each of the members. The other is the amount of relative movement or interfacial sliding occurring between the two pieces.

Milner and Rowe¹¹ indicate that early investigators postulated that surface oxide film breakup was the controlling factor in solid phase welding. These investigators indicated that a critical amount of deformation was needed to produce enough interfacial extension or elongation to produce film rupture. Tylecote¹², p. 24, indicates that the postulates have been shown to be invalid since the oxides have been shown to break up long before bonding occurs. However, there is a critical amount of interfacial extension required to initiate welding. This critical or threshold of interfacial extension

appears to be independent of the method used to produce it. This was shown by an investigation conducted by Agers and Singer¹³. They indented sheets of aluminum of equal thickness using opposed small tools that result in plane strain conditions and found that a 40 percent interfacial extension was required to initiate bonding regardless of prior history or the ratio of tool width to aluminum strip thickness. These results were compared to the height reduction needed to bond aluminum and other metals by other methods. They found that roll bonding and indentation by small circular tools required 3 to 10 times more height reduction than plane strain tools but that the interfacial extensions for aluminum were again approximately 40 percent. They therefore concluded that it was not the amount of height reduction that should be used as a criteria to produce good welds, rather the amount of interfacial extension was the fundamental factor. Measurements for these extensions were obtained through the use of markers scribed on the materials to be joined or by the use of a brittle dyed oxide (aluminum).

It seems from these experiments that a critical amount of surface elongation accompanied by high normal forces is one of the ways clean metal surfaces can be joined. The critical amount of elongation is more than what would be required to break up an oxide on the surface. This may explain why gold, though it is free of an oxide, does not bond much more readily than other soft metals. Tylecote¹², pp. 120-206, reports that a 17 percent reduction in height is

required to roll bond gold at room temperature while indium and lead require only about 10% reduction in height using small circular tools. It must be remembered that working at room temperature for lead and indium corresponds to hot working conditions for these metals.

Milner and Rowe¹¹ indicated that the effects of interfacial sliding were dependent upon the mating materials, i.e., materials that harden during seizure could exhibit some "plowing" of the sliding members while softer materials tend to seize and roll over. Anderson's⁸ work with gold and gold against copper indicate that seizure causes the surface to obtain a turbulent rippled texture. The supposition that softer metals seize when high normal stresses and tangential stresses are imposed, followed by turbulence and rippling if further relative motion occurs, is supported by the studies performed by Joshi¹⁴ on ultrasonic bonds. These studies indicated that interfacial sliding was not necessary for the formation of ultrasonic bonds since the peak-to-peak displacements did not show any discontinuity between the two members during joining.

Another factor affecting the quality of the bond is the local structural changes occurring near the interface, especially under hot working conditions. Milner and Rowe¹¹ indicate that bonds made at elevated temperatures and cooled relatively slow, recover and recrystallize, although the time required for the recrystallization (during or after bonding) has not been reported.

Other structural factors that could contribute to bond quality are voids at the interface and grain boundary migration.

The deformation that occurs during industrial thermocompression bonding operations, as described by Clark⁴, Coucoulas⁵, and Deutsch⁶, for example, is complex. However, all of the methods appear to induce high normal stresses and high shear stresses along the bond interface. In the present investigation, thermocompression bonding was studied by compressing a tape against a gold plated substrate using a flat thermode. This results in plane strain deformation of the two members. Plane strain deformation was used in the present investigation because it is similar to the deformation that occurs in industrial practice, induces high normal and shear stresses at the interface, and is comparatively simple.

Silver markers, plated into grooves etched into the tape surface, were used to indicate macroscopic deformation occurring at the interface. Optical and scanning electron microscopy was used to evaluate microscopic deformation occurring at the interface and structural changes in the two pieces. Geometric effects were explored by varying the thickness of the gold plating on the rigid substrate. In some cases, the bonding operation was interrupted to investigate the chronological development of deformation and of bond formation.

II. EXPERIMENTAL PROCEDURE

The deformation occurring at the interface between two gold parts joined by thermocompression bonding was investigated using a marker technique to determine macroscopic movements and using scanning electron microscopy to estimate topographic changes. In all of the experiments, one of the gold parts was a tape measuring 0.254 mm (0.010 in) x 1.575 mm (0.062 in) x 9.526 mm (0.375 in) and the other part was gold plated onto a rigid steel substrate. The tape was bonded to the substrate gold by pressing the parts together between two flat and parallel thermode faces heated to the same temperature. In one series of experiments, the thickness of gold plated on the substrate was varied. The effect of substrate gold thickness on deformation occurring at the interface was determined at 573°K (300°C) and at 643°K (370°C) with the applied force adjusted so that the resulting reduction in height during bonding was approximately 15%. The force was applied for a total of six seconds in all of the thickness variation experiments. The chronological development of deformation was determined in a second series of experiments. In these experiments, the substrate gold was nominally 0.01143 mm (0.00045 in) thick, temperature was 573°K and force was 3558 N (800 lbs), and the development of height reduction and deformation at the interface was determined by varying the time that the force was applied. The equipment, instrumentation, substrate preparation, and tape marker generation and preparation was the same for the two series of experiments.

Commercially available shim stock of spring-tempered tool steel (Starret), cut into 0.635 mm (0.025 in) x 12.7 mm (0.500 in) x 19.05 mm (0.750 in) pieces, was used as the substrate material because of its rigidity, flatness, and low heat capacity. Gold was deposited on one side using a phosphate type gold plating bath and a 99.999% pure gold anode. Details of the bath composition and its operation can be found in Appendix A. The gold thicknesses for all of the plated substrates generated for this investigation are given in Table 1 and were measured at the step created by the plating fixture (see Fig. 1) using a Leitz split beam microscope. These thicknesses were verified by measurement on photomicrographs of the sectioned samples. The plated gold substrates were not given any heat treatment. However, just prior to bonding, the as-plated gold surface was rinsed with acetone, followed by ethyl alcohol and dried with nitrogen gas.

The tapes used were cut to a length of 9.53 mm (0.375 in) from the same piece of 1.606 mm (0.0625 in) wide by 0.254 mm (0.010 in) thick rolled ribbon stock of nominally 99.999% pure gold, purchased from Englehard Inc., Newark, New Jersey. To insure a uniform starting material for all specimen tapes, an investigation into the effects of annealing temperature on hardness was conducted. Fig. 2 shows the as-received microstructure of the ribbon. As seen by the rounded edges, the final shape was obtained by rolling a round wire into the flat ribbon. The ribbon from which all specimen tapes were cut was annealed for 30 minutes at 473°K (200°C) in air. The results of the

annealing investigation, as shown in Fig. 3 and Table 2, indicate that this treatment should recrystallize the gold. Fig. 4 shows the resulting microstructure. Comparison with ASTM non-ferrous grain size standard indicates that the average grain diameter is approximately 0.018 mm. A tape whose width is about six times its thickness was chosen because it corresponds to the nominal width to thickness ratio of leads on beam leaded integrated circuits.

Markers were generated by depositing silver into 0.0254 mm (0.001 in) wide and 4 μ m deep grooves etched into the tapes on 0.3028 mm (0.012 in) centers as shown in Fig. 5. Markers were produced only on the surface of the tape that contacted the substrate during bonding. Details of the process used to etch the grooves are given in Appendix B. The silver plating bath composition and procedures are described in Appendix C.

A Keller Lab bonder, modified by the installation of high-volume, fast-actuating control valves, was used to produce the bonds for this investigation. The use of these new valves necessitated contacting the upper thermode with the workpiece prior to initiation of the bond cycle, to eliminate impulse loading. It can be seen in Fig. 6, rise and fall times on the order of .040 seconds for loads up to 3870 N (870 lbs) were obtained. These fast rise and fall times are especially important for the series of experiments where dwell times were varied. Both thermodes were fabricated from type 303 stainless steel and a cartridge type heater was installed

in each as shown in Fig. 7. The temperature of each of the thermodes was controlled by its own temperature controller with the control chromel-alumel thermocouples sandwiched between the cartridge heating elements and the thermode. To reduce the thermal gradient between the two thermodes, each was set to the desired interface temperature. The temperature at one of the interfaces was independently calibrated by placing a chromel-alumel thermocouple on the surface of a thermode, separating the thermodes by a 3.175 mm (0.125 in) thick asbestos section, and applying force to the upper thermode. The calibration couple was moved to the other side of the asbestos to calibrate the surface temperature of the other thermode. A strip chart recorder was used to monitor this thermocouple while bringing the monitored thermode to the desired temperature. It was verified that when the controllers were adjusted so that the surface temperatures were the same, the surface temperature also corresponded to the specimen temperature. Both of the thermodes were monitored prior to every bond. The applied load was instantaneously measured by a Statham 4447 N (1000 lb) load cell assembly placed in series with the pneumatic cylinder and the upper thermode. The output of the transducer and its associated read-out were calibrated using a Dillon force gage. A Hewlett-Packard linear transformer type displacement transducer was used to measure the instantaneous sample height during the bond cycle. This displacement transducer and its core were mounted near the thermodes, thus eliminating most of the elastic

deflection of the bonder and fixtures. The outputs of the force transducer read-out unit and the displacement transducer were displayed on a dual-trace oscilloscope. Fig. 8 shows a photograph of the displayed results for a typical bond.

Tapes were bonded to substrates at 573°K (300°C) and 643°K (370°C) using 3870 N (870 lbs) and 3024 N (680 lbs) total applied force respectively and quenched in ice water immediately at the end of the bond cycle. To insure that a uniform sticking friction was obtained from sample to sample, thin gold (approximately 1 μ m) was plated onto steel shim stock and used as the contacting upper platen. All samples were measured with a micrometer to verify the height change indicated by the displacement transducer output displayed on the oscilloscope.

Prior to any sectioning, the steel substrates were etched away from the gold metallization using a 50% water and 50% HCl (by volume) solution heated to 370°K (97°C). Etching the steel was necessary because of the preferential etching of the steel and cathodic protection of the gold when etched. Both sets of samples were sectioned and photomicrographs were taken with the marker generation mask placed over the specimen as a reference for marker movement (Fig 9). The microstructure was observed on all samples optically and using scanning electron microscopy. The polishing techniques used in this investigation are in Appendix D. One-half the length of the tapes bonded at 573°K (300°C) had 40 nm (400 Å) of carbon deposited

on them to inhibit bonding. The tapes were separated and scanning electron microscopy was used to qualitatively evaluate the topographic changes occurring during bonding.

The second series of experiments for this investigation, involving interrupted bonding times, used tapes coated with 20 nm (200 Å) of carbon to inhibit bonding and had markers generated on the bonding side. A Lektra Electronic Decade interval timer was used to energize the control valves for the pneumatic cylinder and can vary bonding times from .1 to 111 seconds in .1 second intervals. The particular bond times used were: 0.1, 0.2, 0.5, 2.0, and 6.0 seconds. Again, an oscilloscope was used to record the force and reduction in height vs. time. The tapes were separated from the substrates and both scanning electron and optical microscopy was employed to estimate the topographic changes. By using the marker generation mask aligned on the tapes, marker movement was measured for a given thickness as a function of time. The results of these marker motion measurements and observed topographic changes and those of the first series of experiments are given in the next section.

III. RESULTS AND DISCUSSION

The specimens for the substrate thickness variation investigation were metallographically prepared by sectioning and etching. Photomicrographs were taken to observe both the marker motion and the microstructure as shown in Figs. 9, 10 and 11.

Each specimen had the marker generation mask superimposed on it so that original marker spacings could be observed, as shown in Fig. 9. The interfacial deformation was analyzed by plotting the marker motion (ΔL) as a function of original marker distance from the center of the tape (L). To plot the data, it was assumed that the interfacial motion was symmetric about the center of the tape. These marker motion measurements are presented in Figs. 12 and 13 which are for bonding temperatures of 573°K (300°C) and 643°K (370°C), respectively. There was some specimen to specimen variation in height reduction and bond force as given in Table 1. The marker measurements were normalized to a nominal 15% deformation by multiplying the actual marker motion, ΔL , times the ratio $0.15/d$. The deformation, d , is defined by:

$$d = 1 - \frac{(p+h)_f}{(p+h)_i}, \quad (1)$$

where $(p+h)_f$ is the sum of the substrate plating thickness (p) and the deformed tape height (h) after deformation and $(p+h)_i$ is the initial sum. The normalized marker motion measurements, $\Delta L (0.15/d)$, are plotted as a function of the substrate thickness ratios, $p_i/(p+h)_i$, in Fig. 14. The family of curves corresponds to different fractional distances from

the center as expressed by the ratio L/L_t where L is the distance from the center and L_t is the initial total distance from the center or one-half the original tape width. As can be seen from this data, the deformation mode does not appear to be temperature dependent over the range of metallization thicknesses evaluated. There appears to be some discrepancies for low $p_i/(p+h)_i$ ratios which could be due to erratic sliding of the tapes on the thinner substrates.

It would be convenient to compare curves of normalized marker motion as a function of position so that the effect of different substrate thicknesses would be clearly indicated and not be confused by slight differences in total deformation. Such a normalized set of marker motion data was taken from the curves in Fig. 14 and are plotted in Fig. 15. It is seen that the curves in Fig. 15 are well behaved after accounting for the variations in total deformation using the normalization procedure.

One of the parameters of interest in bond formation is the amount of surface elongation. The conventional or engineering concept of unit strain will be used to define strain at a surface as given by:

$$e_s = \frac{\Delta L}{L} \quad , \quad (2)$$

where ΔL is the change in length of some portion of the surface of original length L . If the elongation were uniform along the surface, ΔL and L would correspond directly to marker motion and original marker position for the present experiments. For these experiments,

it is more appropriate to consider the strain over some small increment of surface and define the tape surface strain by:

$$e_s = \frac{d(\Delta L)}{d(L)} \quad , \quad (3)$$

where ΔL now corresponds to the motion of some marker in the tape which was originally a distance L from the center (where ΔL is zero). Surface strain, e_s , as defined by Equation (3), was determined by measuring the slopes of the normalized ΔL vs. L curves of Fig. 15 and are plotted in Fig. 16.

The strains at the edge of a tape specimen, for a given amount of deformation, appear to remain constant for all values of substrate thicknesses investigated. However, it is seen that strains nearer to the center are quite dependent on the ratio of substrate plating thickness to the total height, $p_i/(p+h)_i$. For relatively thin substrate plating thicknesses or for relatively thick tapes or leads, there is no surface elongation in the region near the center of the bond. On the other hand, for relatively thick substrate plating thicknesses, or for relatively thin tapes or leads, there is even greater surface elongation in the central region of the bond than near the edge..

Another parameter that may be of importance to the formation of a thermocompression bond is the amount of interfacial sliding. Interfacial sliding is the displacement of one of the members to be bonded relative to the other. At some point at the interface, a distance L

from the center, the amount of interfacial sliding can be defined by:

$$\delta_s = \Delta L - \Delta L_p, \quad (4)$$

where ΔL corresponds to the marker motion measurements and is the displacement of a point originally on the surface of the tape or lead a distance L from the center and ΔL_p is the displacement of a point originally on the surface of the plated substrate also a distance L from the center of the bond region. This definition of δ_s is shown schematically in Fig. 17. Consider the case of thin substrate plating well adhered to rigid steel shim stock. In the extreme case where p approaches zero, ΔL_p would also have to be zero and δ_s would correspond to the measured marker motion ΔL . The amount of interfacial sliding can be estimated by extrapolating the curves of ΔL vs. $p_i/(p+h)_i$ of Fig. 14 back to $p_i/(p+h)_i = 0$. It is seen that for L/L_t ratios of 0.4 or less, the curves clearly extrapolate to zero or nearly zero. In other words, there appears to be no interfacial sliding near the center of the bond region. This is as expected since there are high normal stresses in the region and low shear stresses. At higher L/L_t ratios and low $p_i/(p+h)_i$ ratios, the scatter in the marker motion measurements is assumed to be due to erratic stick-slip sliding. The dashed curves of Fig. 14 were used to estimate the amount of surface sliding in the regions near the edge where normal stresses are lower and sliding would be expected. The estimate of surface sliding, δ_s , corresponds to the $p_i/(p+h)_i = 0$ curve

of Fig. 15. This would also be expected to be an upper bound on the amount of sliding occurring at higher $p_i/(p+h)_i$ ratios (thicker plating) since the shear stresses induced at the interface would be lower.

Though motion of the plated surfaces was not measured using markers, the motion can be estimated from the distortion of columnar grains that is apparent in Fig. 10. Figs. 18 and 19 are higher magnification views of specimens with $p_i/(p+h)_i$ of 0.246 and 0.281 respectively showing a marker designated "4" near the edge of the tape where sliding would be expected to be highest. The initial position (before bonding) is known from the ΔL measurements and is designated "1". If there were no sliding, an original vertical line connecting "1" and "5" would deform and form a curved line between "4" and "5". If there were sliding equal to that estimated at $p_i/(p+h)_i = 0$, the originally vertical lines would have deformed to a curved line connecting "3" and "5". The distance between "3" and "4" then corresponds to the assumed δ_s and the distance between "1" and "3" corresponds to the plated surface motion ΔL_p . The dashed curves connecting "2" and "5" in Figs. 18 and 19 are what the author estimates as the deformation occurring in the plated material. These estimates and others then indicate that δ_s does not vary significantly with plating thickness or the $p_i/(p+h)_i$ ratio. By assuming interfacial sliding, a lower bound estimate of plated substrate elongation, $\Delta L_p(0.15/d)$, was obtained by subtracting the curve for $p_i/(p+h)_i = 0$ from the remaining curves of Fig. 15. These lower bound estimates of ΔL_p are plotted

on Fig. 20. From Equation (4) it can be seen that the upper bound of ΔL_p occurs when it is assumed that there is no sliding ($\delta_s = 0$) and then ΔL_p is identical to ΔL . For low L/L_t values, there is little difference between the lower and upper bound estimates and ΔL_p is approximately equal to ΔL since there is no sliding.

The amount that the plated surface on the substrate elongates is another parameter of interest. If surface elongation is important to thermocompression bond formation, then presumably the surface with the least elongation would exert the dominating influence. Since any sliding that occurs reduces the amount of elongation of the thinner member, the elongation of the substrate plating would be expected to be important.

The strain at the plated surface is defined by:

$$e_p = \frac{d(\Delta L_p)}{d(L)} \quad , \quad (5)$$

where ΔL_p is the motion of a point on the plated substrate surface that was initially a distance L from the center of the bond region. As has already been discussed, if there is no sliding, the motion and also the surface strain would be identical for the tape and for the plated substrate. A lower bound estimate of the strains at the plated surface was obtained by differentiating the curves of Fig. 20 and are presented in Fig. 21. The lower bound estimates of the strain on the plated surface approach zero near the edges of the sample. The lower

bound estimates would imply though, that there is considerable sliding in these regions. The upper bound estimate on the other hand, predicts strain values approaching some constant value for high L/L_t . The plated surface elongation would be identical to the elongation of the tape and unaccompanied by sliding. In other words, these experiments indicate that in the bond regions near the edge of the tape there is either (1) considerable surface elongation of both the tape and the plated surface, (2) considerable relative motion between the two surfaces but perhaps no surface elongation of the plated surface, or (3) a combination of sliding and elongation of the plated surface.

The surface parameters are interdependent as can be seen from Equation (4), so less sliding is accompanied by more motion of the plated surface for a given amount of tape surface motion. As the metallization thickness becomes an appreciable fraction of tape height, the strains at the center of the bond interface become large. This holds true for either the upper or lower bound estimates.

All of the preceding discussion has assumed that the interface remains planar. This appears to be a good approximation on a macroscopic scale. There is some variation in plating thickness that is apparent after bonding onto the thicker substrate platings as can be seen in Figs. 9 and 10. However, this slight distortion of the interface is not enough to introduce measurable errors. On a microscopic scale though, there is surface "rippling" which makes an

interfacial extension contribution that is not detected by analysis of marker motion. "Rippling" is evident, for example, between the last two markers on the left in Fig. 10. The "rippling" exhibited a strong substrate plating thickness dependence that was apparent from both optical and scanning electron photomicrographs. The amplitude and the wavelength of the "ripples" were smaller for thinner substrate platings. The scanning electron photomicrographs taken of the substrate and tape surfaces, bonded at 573°K (300°C) with carbon on the surface, clearly indicated increased "rippling" for thicker substrate platings. The thicker substrate platings also exhibited some finer scaled long and parallel "ripples" presumably due to the penetration of slip lines. The slip line penetration was more prevalent towards the edges of the tapes. Both the surface "rippling" and the slip line penetration result in surface extension in addition to the surface strain detectable by marker motion. These microscopic surface extension mechanisms appeared to be more prevalent in the regions nearer the edges of the tapes.

Examination of Fig. 11 shows that both the tape and the substrate plating have recrystallized after bonding when the sample is allowed to air cool. However, those samples that were quenched immediately after bonding did not show complete recrystallization as can be seen by Figs. 9 and 10. It should be pointed out that the steel shim stock substrate has a lower heat capacity than usual substrate materials of either ceramic or glass. With conventional substrate materials and

bonding operations, cooling would be even slower than the air cool of these experiments and recrystallized structures would certainly be expected.

Scanning electron micrographs were taken across all of the sectioned interfaces at magnifications of at least 500X. Examination of these micrographs indicated that occasionally grain boundaries migrate across the bond interface. Fig. 22 is a 3000X micrograph of an unquenched sample that had been bonded at 643°K (370°C) and shows several areas where grain boundaries migrated across the interface. For the thinner substrate platings, grain boundary migration was only observed in the bond regions near the edges. The frequency of these interfacial crossings was dependent on the substrate thickness, i.e., as the thickness increased the frequency increased and the position, L/L_t , at which they first cross approaches zero. There was no noticeable difference in the frequency of grain boundary migration across the interface for the two bonding temperatures.

Preferential etching was generally observed at the bond interface. In regions where grain boundaries had not migrated across the surface, there would be lattice mismatch across the interface because of different grain orientations. An etch rate at least as fast as grain boundary etching would be expected even if the bond was perfect. Generally, the bond interface joining two differently oriented grains etched faster than grain boundaries. There was usually preferential etching at the interface even if a grain boundary had migrated past as

can be seen in Fig. 22. Figs. 23 and 24 are micrographs of the bond interface that is within a single grain. A twin runs from the upper side of the micrograph to the right of center down through the original interface. It is seen that there is still preferential etching. There also appear to be some voids. There were sometimes interface regions within a grain which did not preferentially etch enough to be visible. An assumption of a distribution of void sizes remaining at the bond interface due to incomplete conformity appears to be compatible with all of the observations. A high density of voids would impede grain boundary migration. A lower density would allow grain boundaries to sweep around the voids. Voids remaining at the original interface would provide high corrosion paths during etching but should be passive otherwise.

The interrupted bonding experiments had erratic marker motion. Presumably the carbon present on the surface inhibited seizure and resulted in unreproducible amounts of sliding. Qualitative analysis did indicate a dwell time dependence on the amount and position distribution of surface "rippling". As the dwell time increased, the "rippled" surface percentage increased with the observable position where "rippling" was initiated tending towards $L/L_t = 0$.

The final heights of specimens bonded as part of the interrupted bonding studies are plotted on Fig. 25 along with the change in height as a function of time that was indicated by the oscillograph of a six second dwell time specimen. All specimens had about the same plating

thickness though the force varied slightly from test to test due to air pressure regulation. It is seen that correlation is good if the difference in forces is accounted for.

Some interrupted bonding experiments were performed without carbon present to inhibit bonding. These specimens bonded well enough that they could not be pulled apart. One of these bonded specimens had a 2980 N (670 lb) bond force imposed for only 0.4 seconds at 643°K (370°C) which resulted in a four percent reduction in height. The surfaces of specimens from the interrupted bonding experiments, performed with carbon present, were examined. The scanning electron micrographs indicated that conformity and asperity deformation developed at about the same rate as the height of specimen was reduced. In other words, a considerable portion of the asperity deformation occurs in the first fractions of the bonding time. A considerable portion of the surface elongation and sliding at the interface would also have occurred and the development of bonds is not surprising.

There is, however, no reason to expect that the amount of surface sliding is proportional to total deformation or occurs simultaneously with surface elongation. It is possible that most sliding occurs in the initial stages of the loading cycle before the bond force has reached its full value. As the normal stresses approach their equilibrium values, seizure could occur. This would prevent further sliding and further deformation would occur by mutual elongation

of the two surfaces. This would explain the smoothness of the force and deformation oscilloscope traces. Erratic force and deformation behavior that would be expected under stick-slip conditions should have been detectable by the instrumentation unless it occurred during the application of the bond load.

The forces required to deform the specimens can also be correlated with plasticity theory. The configuration of tape that was used in these experiments was relatively long so that plane strain conditions can be assumed. It will be assumed that the deformation of the tape and substrate plating can be approximated by the deformation of a homogeneous bar having the same width as the tape and a height equal to the thickness of the tape. This neglects the work required to deform the substrate plating. Since bonding occurred in all of the specimens, sticking friction conditions can be assumed. In this case, the shear stresses at the upper and lower surfaces of the tape are equal to the shear stress, τ , of the material as given by:

$$\tau = \sigma_0 / \sqrt{3} \quad (6)$$

where σ_0 is the flow stress under uniaxial stress conditions.

¹⁵
Avitzur, p. 363, gives an upper bound solution for deformation under these conditions that can be represented by:

$$F = P_{ave} A = \frac{2}{\sqrt{3}} \sigma_0 \left(1 + \frac{w}{4h}\right) \quad (7)$$

where F is the total applied force

P_{ave} is the apparent stress or average pressure

A is the area over which the force is applied

σ_o is the instantaneous flow stress under uniaxial stress conditions

w is the tape width

and h is the tape height.

Figure 26 shows the change in total height of tape and substrate plating as a function of time for four different samples deformed at 573°K (300°C). The curves are not smooth because values were manually read from the oscilloscope traces and are plotted on an expanded scale. The curves are somewhat different because of minor variations in the forces applied. Fig. 27 shows the instantaneous flow stress, σ_o , calculated from Equation (7) for the specimens deformed at 573°K (300°C). It is seen that correlation from specimen to specimen is good. The flow stress decreases with time because the strain rate is decreasing. For example, the true strain rate at .1 seconds is estimated to be about $.17 \text{ sec}^{-1}$. At the end of the six second dwell time, the strain rate has fallen to $.0035 \text{ sec}^{-1}$. Fig. 28 shows similar curves of total height as a function of time for four samples deformed at 643°K (370°C). The instantaneous flow stress, σ_o , corresponding to the deformation of these four specimens is plotted in Fig. 29 and correlation is again good. The instantaneous flow stresses calculated here for 573°K

(370°C) are in agreement with the constant strain rate determinations by Condra¹⁶.

The information that has been obtained from this investigation implies that changes in bonding tool design could be made that would enhance gold to gold, thermocompression bonding. Tool modifications would entail optimization of interfacial elongations with the lead or tape height and plated substrate thickness as boundary conditions.

Total bonding times have been significantly reduced and can be on the order of one second. This reduction is partly the result of the high speed bonder that essentially eliminates the rise and decay times usually associated with industrial bonding.

IV. SUMMARY AND CONCLUSIONS

These bonding experiments were performed under plane strain conditions, but otherwise are similar to industrial thermocompression bonding practice. The use of silver markers to accurately measure the deformation occurring at the interface has been demonstrated. Analysis of marker motion and correlation with observation of metallographic sections defined conditions at the interface that are sufficient for bond formation.

This investigation has shown that a 15 percent reduction in height results in a 12 percent surface elongation in regions towards the edges of the tape and appears to be independent of substrate plating thickness. Bonding occurred throughout the regions where there was tape elongation except at the very edge where normal stresses would be expected to be low. These regions where bonding occurred also have either considerable elongation of the substrate plating surface, sliding, or some combination of plating elongation and sliding.

Surface strains nearer to the center of the bond region depend on the relative thickness of the substrate as expressed by the $p/(p+h)$ ratio. For low $p/(p+h)$ ratios, there was negligible surface elongation in regions near the center and bonding did not occur. For $p/(p+h)$ ratios of about 0.12 and above, surface elongation was 12 percent or more. There appeared to be no sliding in the central region out to about four tenths of the distance to the edge regardless of the relative thickness of the plating.

Quenched specimens did not completely recrystallize indicating that recrystallization is not the dynamic softening mechanism for gold under these conditions. Specimens that were allowed to air cool did recrystallize however. Metallographic examination of the interfaces showed that grain boundaries occasionally migrate across the interface whether the tape and substrate plating have recrystallized or not.

Conditions sufficient to cause bond formation have been determined and the deformation that occurs has been defined. It appears from the present experimental results that markers should be plated on both the tape and on thicker substrate platings to determine the amount of sliding that occurs at the interface. If the amount of sliding and the effect of changing the amount of height reduction is determined, deformation occurring at the interface would be completely defined. This would allow the determination of threshold conditions required for bond formation without the necessity of performing marker motion experiments since the deformation occurring at the interface could be predicted with confidence.

TABLE 1
Tape and Plated Substrate Metallization Parameters

TEMPERATURE	BONDING FORCE	SPECIMEN PARAMETERS (μm)						
		P_i	$(p+h)_i$	w_f	h_f	P_f	$(p+h)_f$	d
573°K (300°C)	3602 N (810 lbs)	2.01	256.02	1793.2	216.97	1.51	218.48	0.146
	3847 N (865 lbs)	11.60	265.05	1770.4	229.58	9.83	243.69	0.084
	3869 N (870 lbs)	25.40	279.40	1779.2	220.12	24.66	245.04	0.123
	3736 N (840 lbs)	65.09	319.09	1798.3	217.22	68.83	281.05	0.151
	3647 N (820 lbs)	82.80	336.80	1788.2	218.95	65.66	284.61	0.155
643°K (370°C)	3002 N (675 lbs)	1.26	255.26	1757.7	220.22	1.01	221.25	0.133
	3091 N (695 lbs)	12.12	266.12	1836.7	213.94	10.34	224.28	0.157
	3046 N (685 lbs)	52.22	306.22	1771.1	218.48	50.96	269.44	0.120
	3024 N (680 lbs)	99.23	353.20	1770.4	218.73	91.63	310.36	0.121

Note: Initial tape width, w_i , 1557 μm (0.0613 in.) and initial tape thickness, h_i , 254 μm (0.010 in.).

TABLE 2
Hardness Values of Annealed Gold

<u>ANNEALING TEMPERATURE</u>	<u>VDPH*</u>
As Received	70.90
373°K (100°C)	73.70
398°K (125°C)	69.87
408°K (135°C)	34.34
423°K (150°C)	33.60
473°K (200°C)	31.42
523°K (250°C)	34.56
573°K (300°C)	32.96

*Vickers Diamond Pyramid Harness - 100 g load.

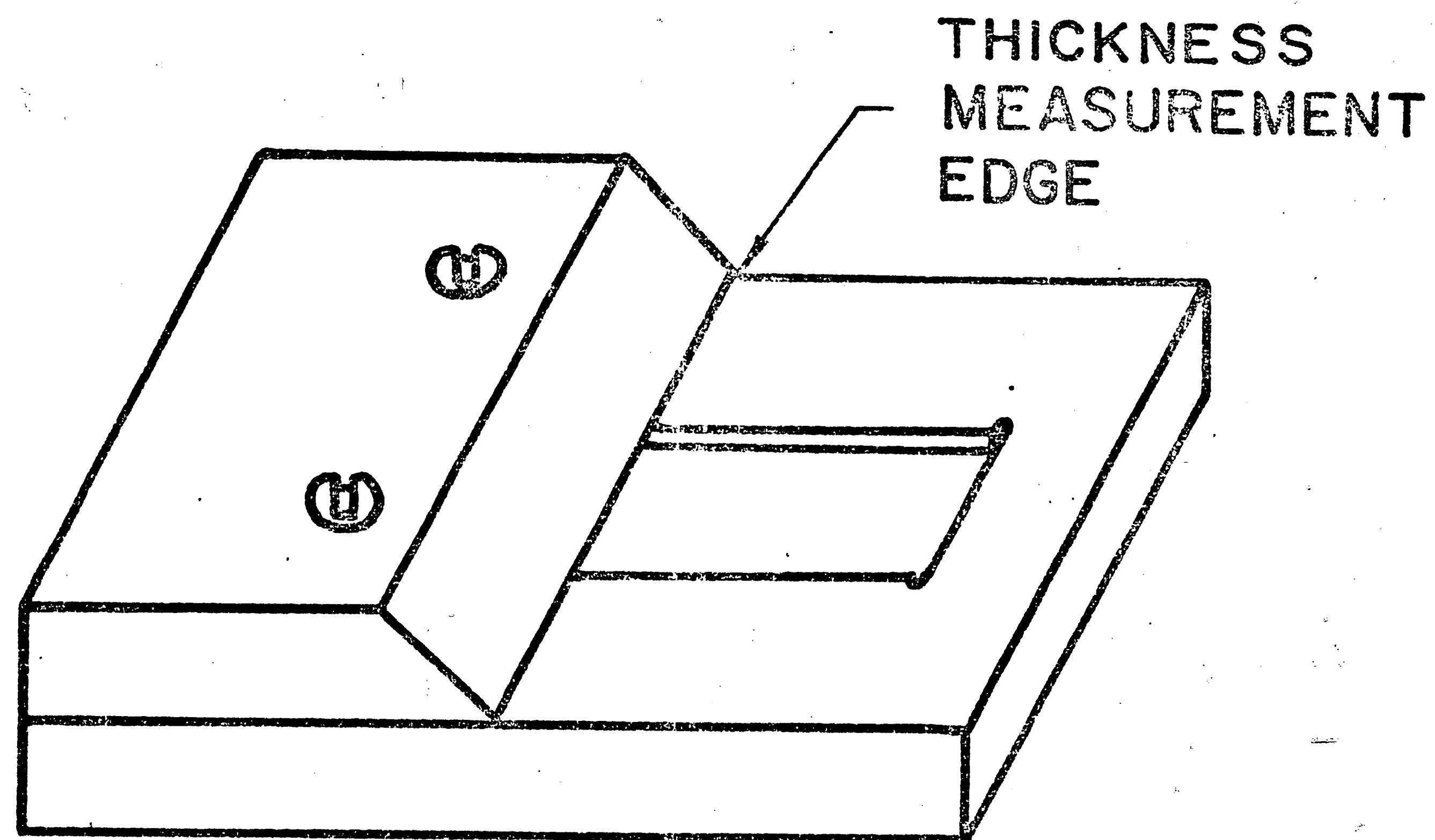


FIG. 1. SUBSTRATE PLATING FIXTURE.

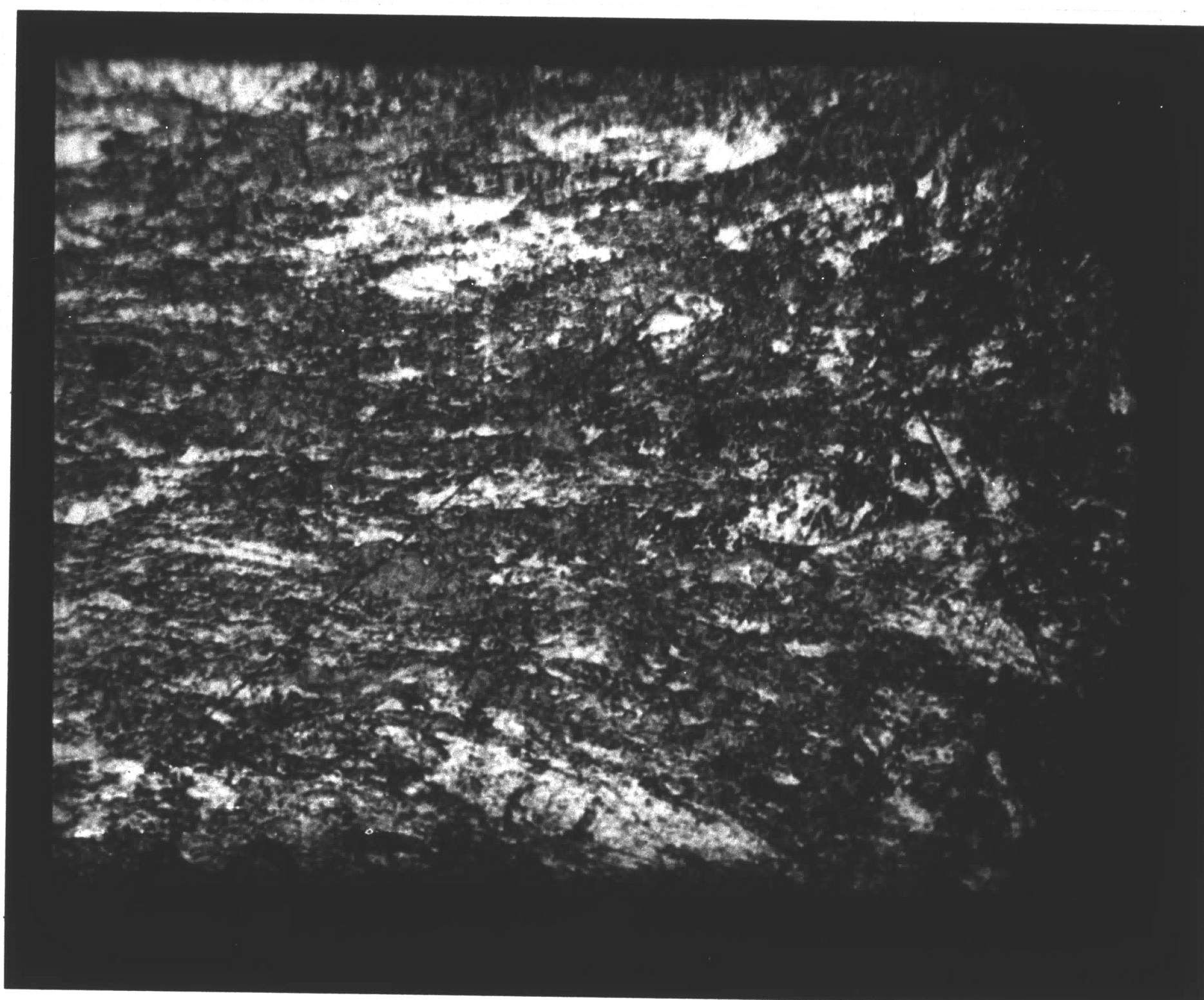


FIG. 2. AS - RECEIVED MICROSTRUCTURE OF GOLD RIBBON
300X.

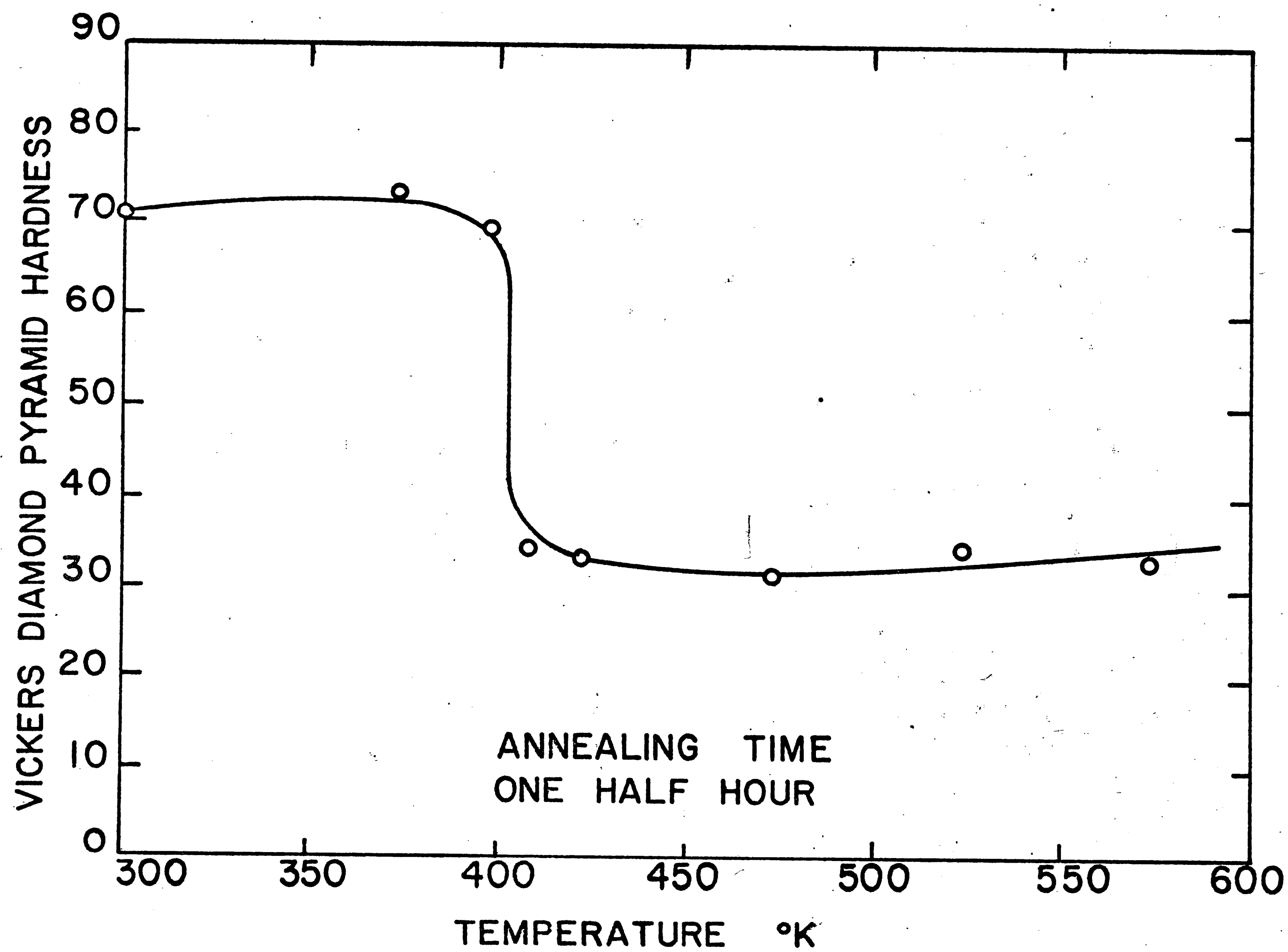
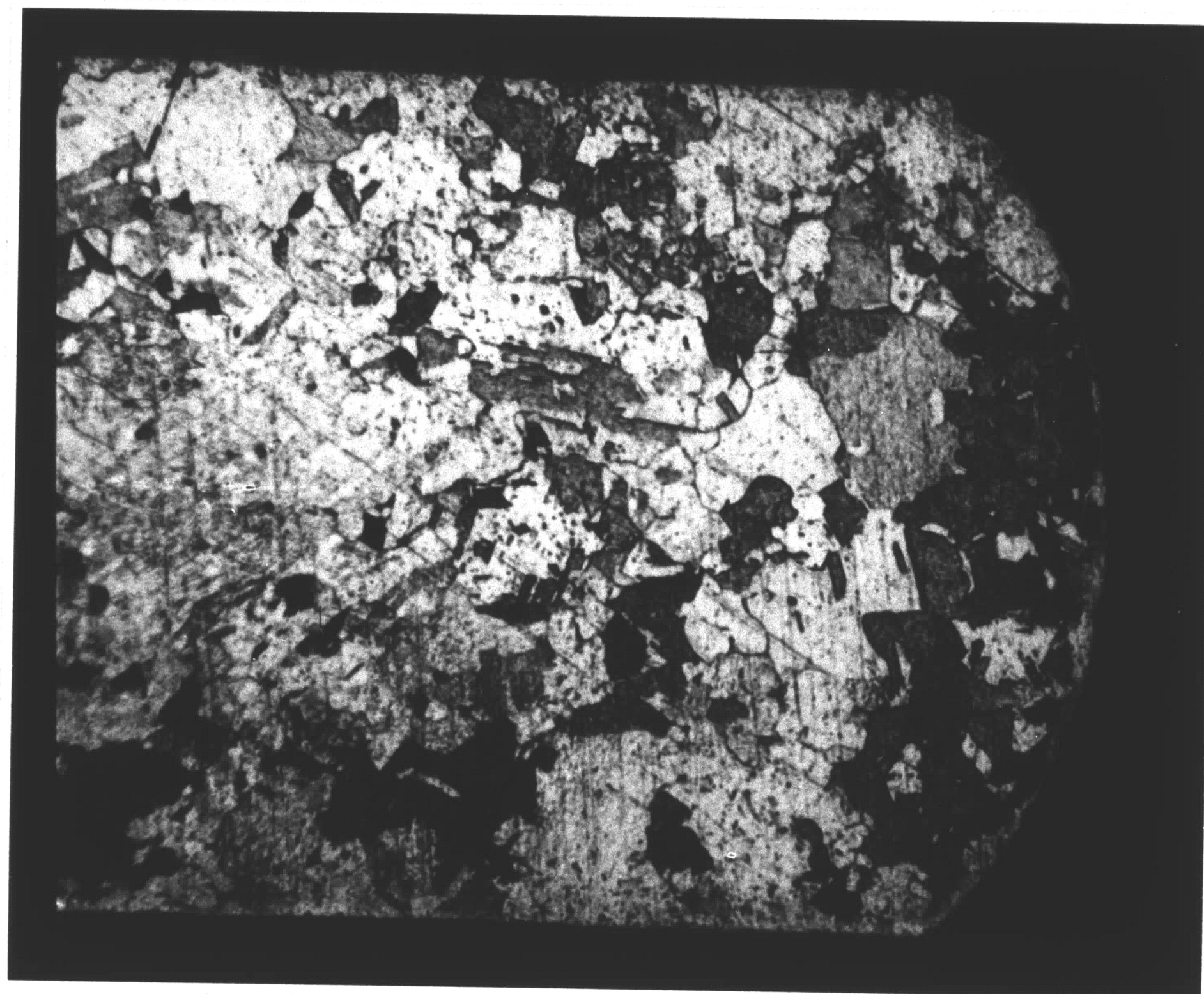
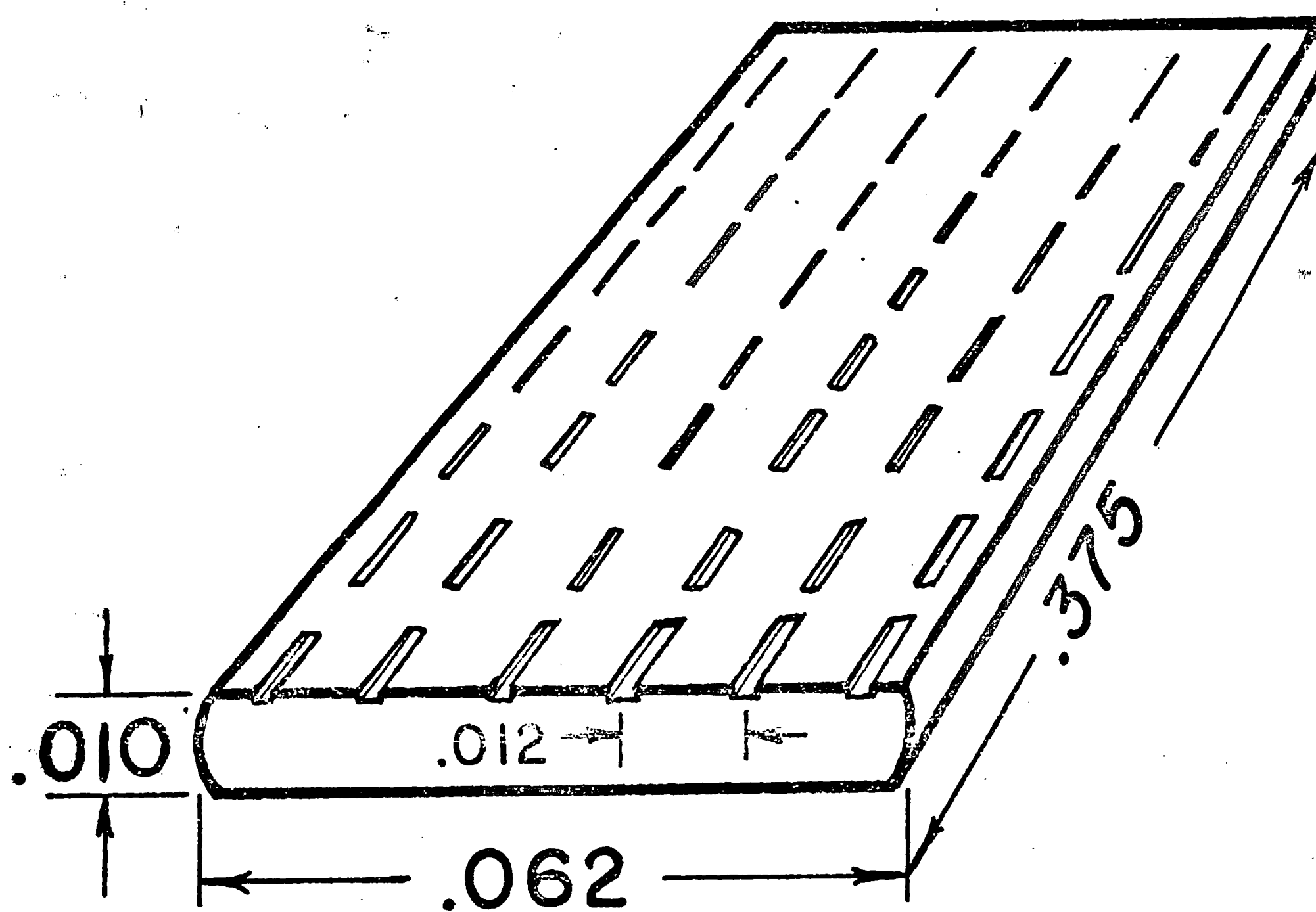


FIG. 3. VDPH MEASUREMENTS AS A FUNCTION OF ANNEALING TEMPERATURE.



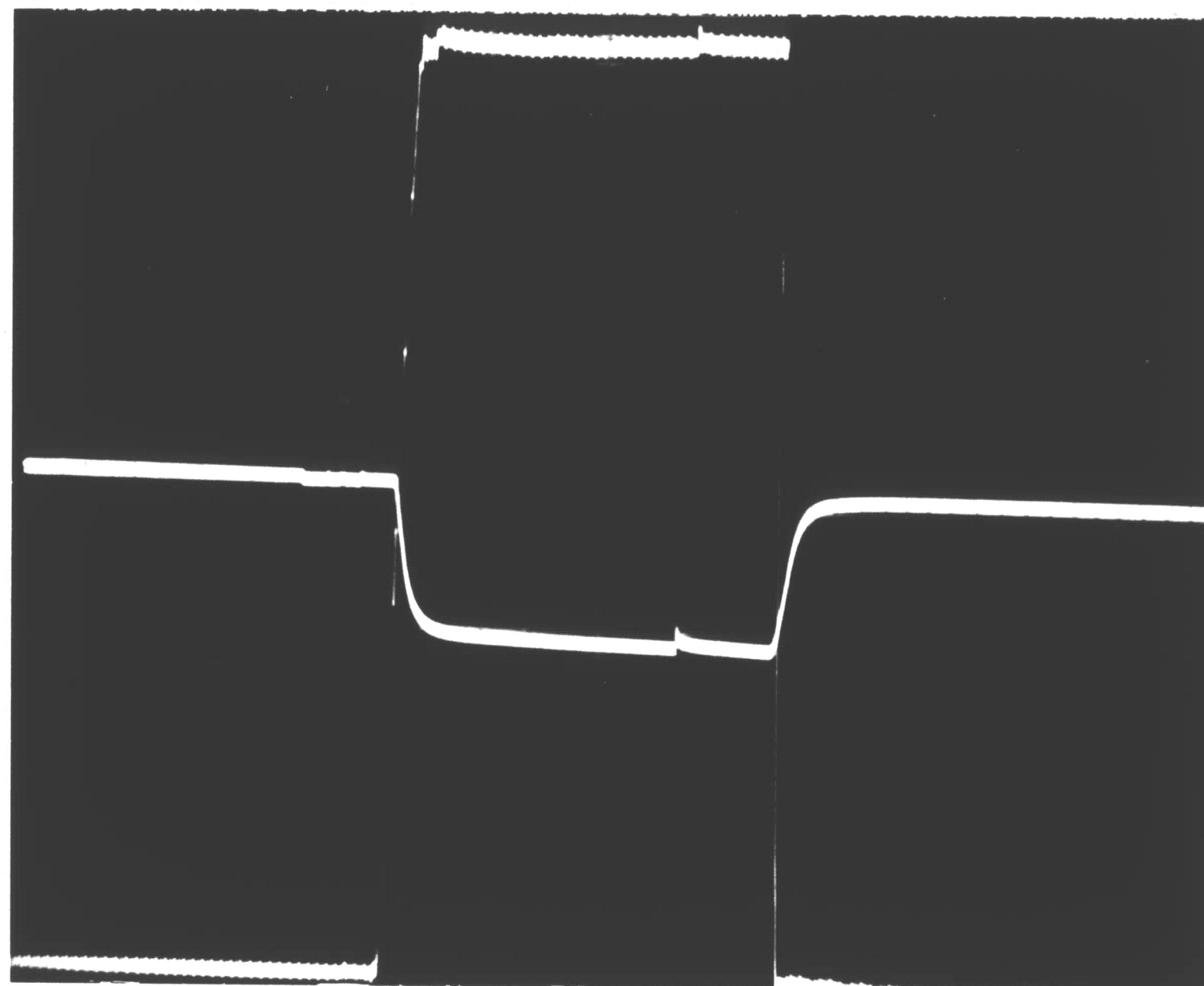
H 3303

FIG. 4. MICROSTRUCTURE OF ANNEALED GOLD RIBBON.
SPECIMEN WAS ANNEALED FOR ONE-HALF HOUR
AT 473°K (200°C).
300X.



PARTIALLY FILLED GROOVES
WITH PLATED SILVER.
(GROOVES .001 in. WIDE and 4 μ m DEEP)

FIG. 5. SCHEMATIC DRAWING OF SILVER MARKERS
IN A GOLD TAPE.



H-3303-A

FIG. 6. TYPICAL FAST RISE AND FALL TIMES FOR
THE MODIFIED KELLER LAB BONDER.
SCALES ARE 445 N (100 LBS)/CM,
25.4 μm (0.001 IN.)/CM AND 0.2 S/CM.

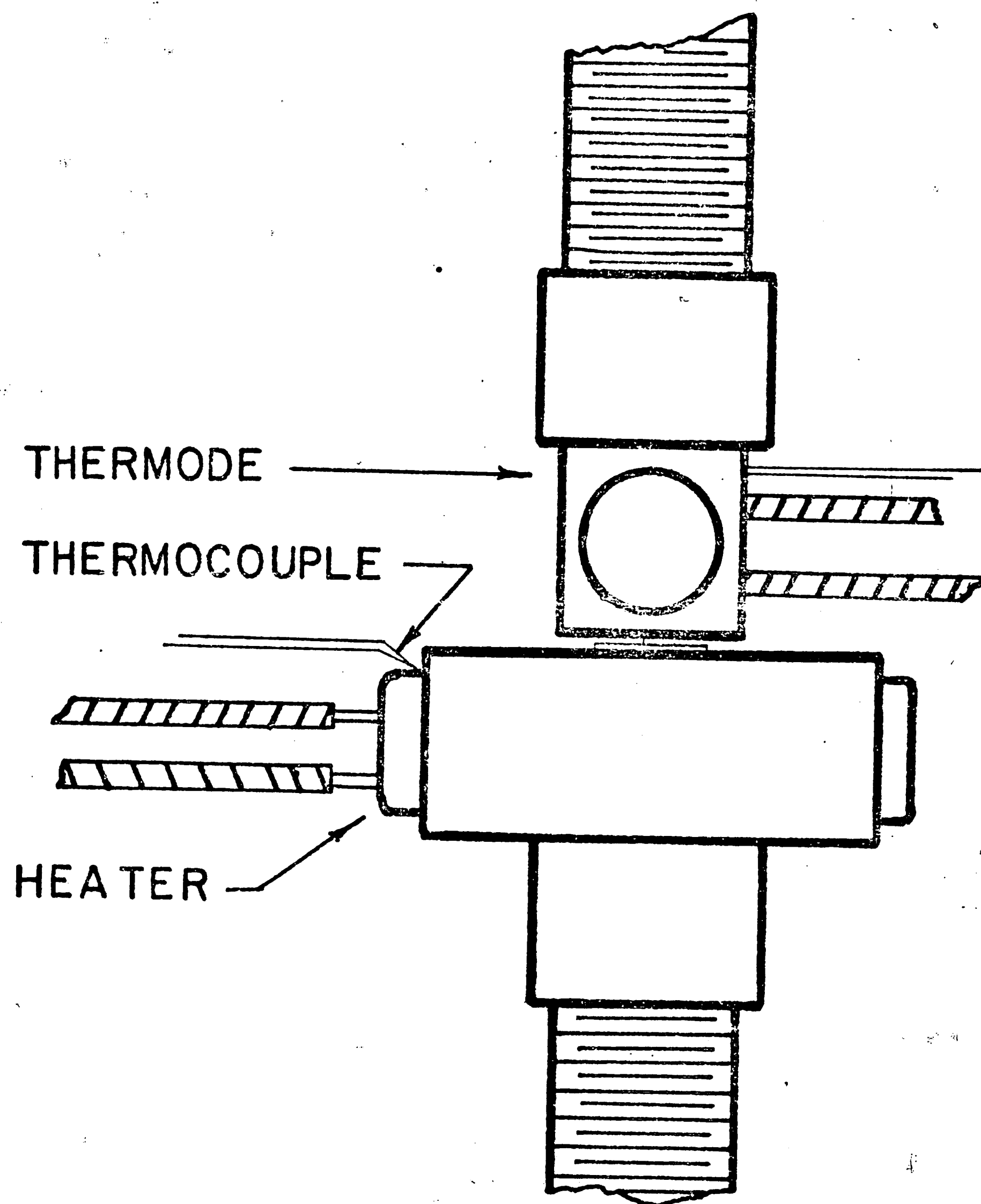


FIG. 7. THERMODE AND HEATER CARTRIDGE CONFIGURATION.



H-33038

FIG. 8. TYPICAL FORCE AND HEIGHT VS. TIME
OSCILLOGRAPH. SCALES ARE 445 N
(100 LBS)/CM, 25.4 μ m(0.001 IN.)/CM
AND 0.2 S/CM.



FIG. 9. PHOTOMICROGRAPH OF SECTIONED TAPE SHOWING SILVER MARKERS AND REFERENCE MASK OVERLAY.



FIG. 10. MICROSTRUCTURE OF QUENCHED TAPE AND PLATED SUBSTRATE METALLIZATION.

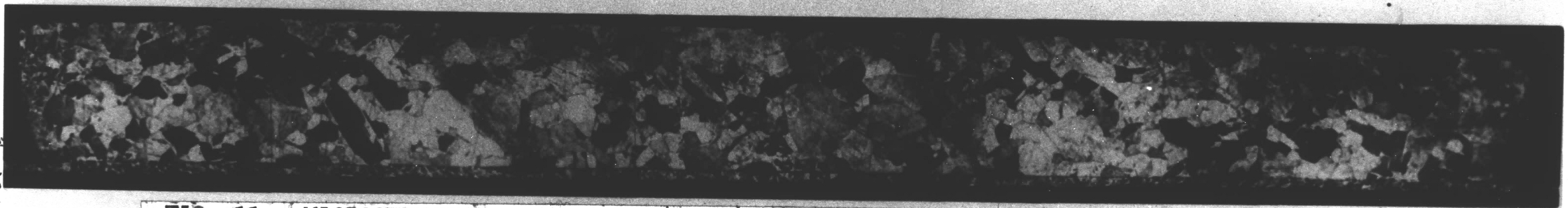


FIG. 11. MICROSTRUCTURE OF AIR-COOLED TAPE AND PLATED SUBSTRATE METALLIZATION.

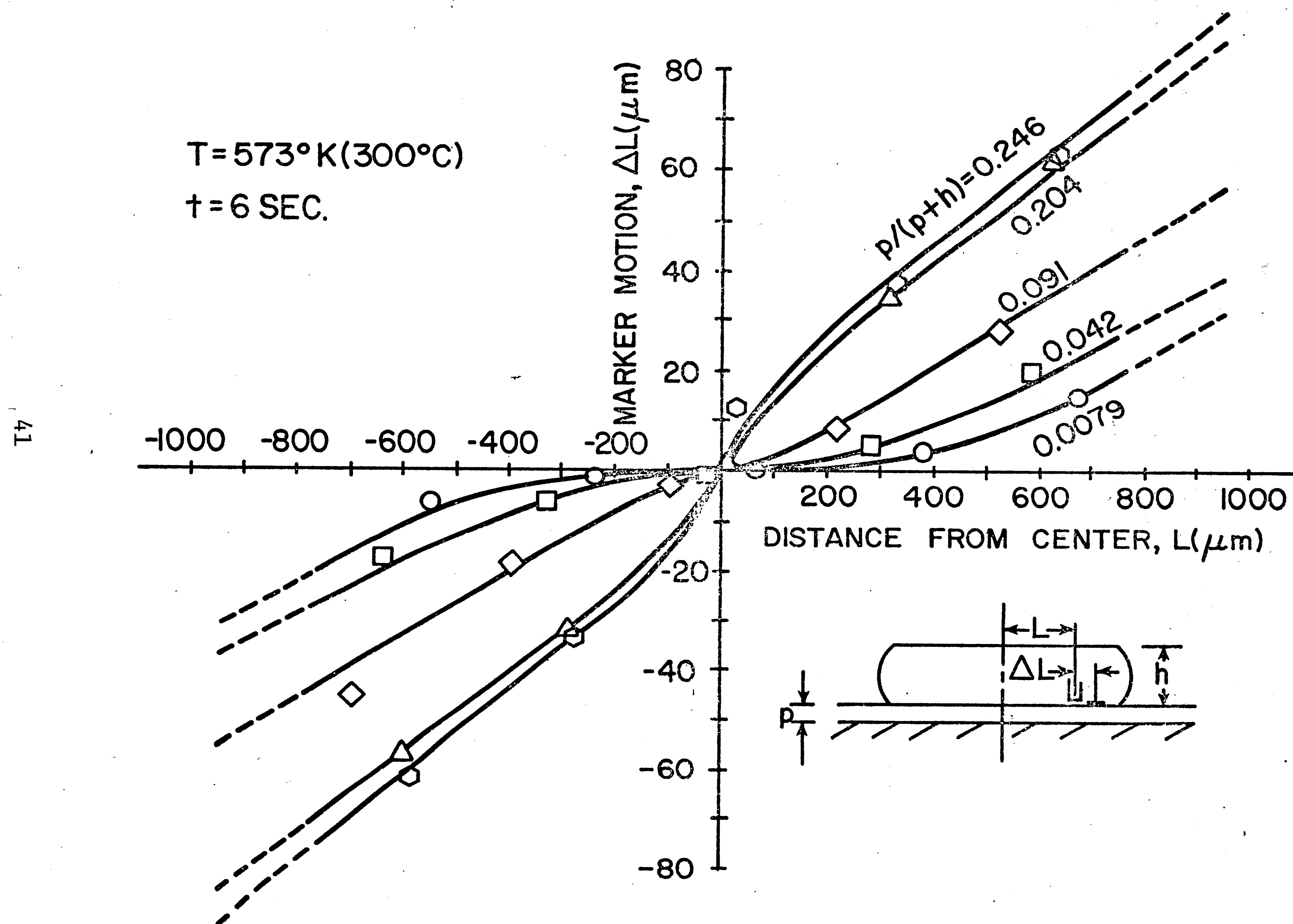


FIG. 12. MARKER MOTION VS. DISTANCE FROM THE CENTER FOR $573^\circ\text{K} (300^\circ\text{C})$. BONDING DWELL TIME WAS 6 SECONDS.

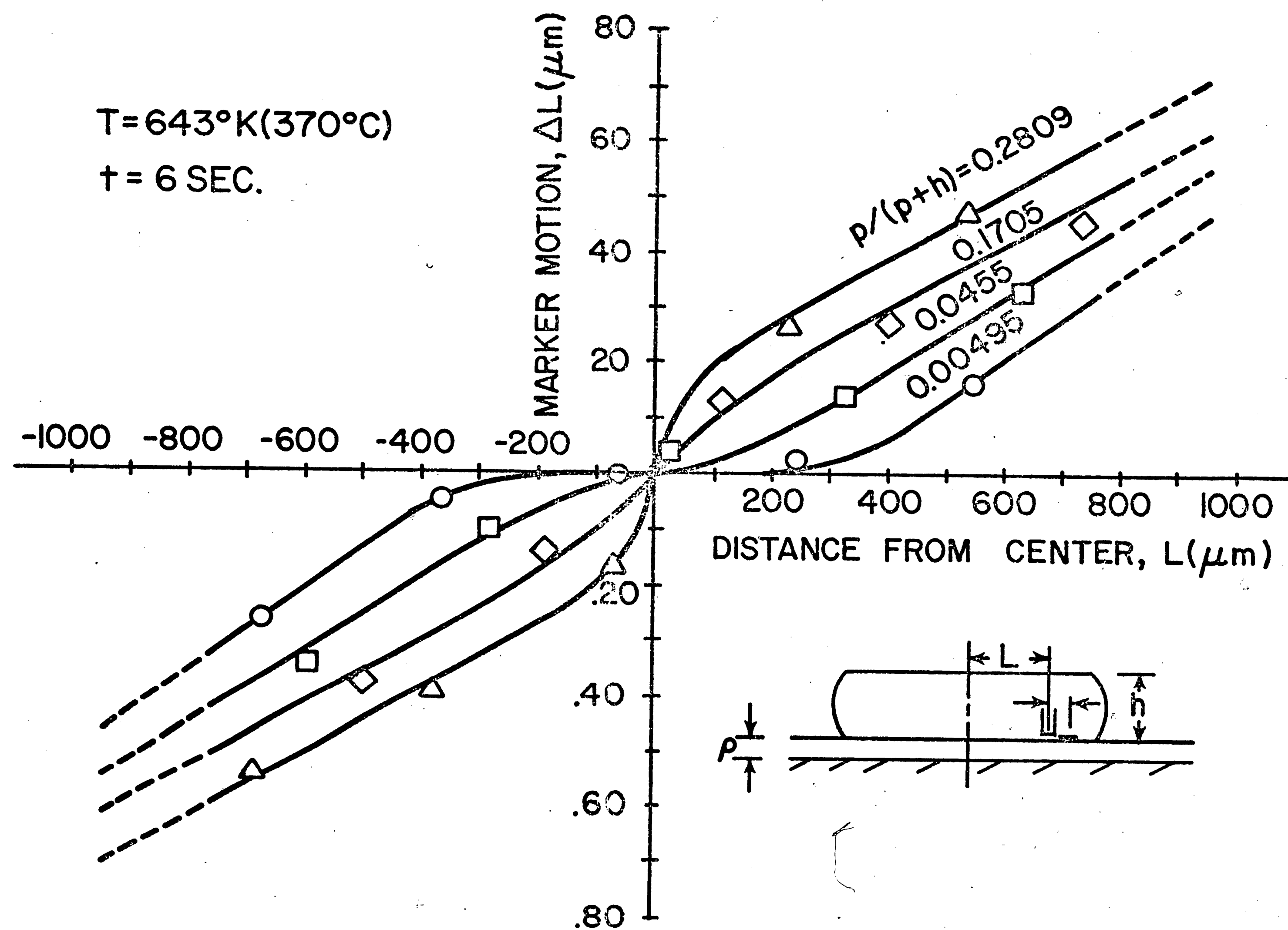


FIG. 13. MARKER MOTION VS. DISTANCE FROM THE CENTER FOR $643^{\circ}\text{K} (370^{\circ}\text{C})$.
 BONDING DWELL TIME WAS 6 SECONDS.

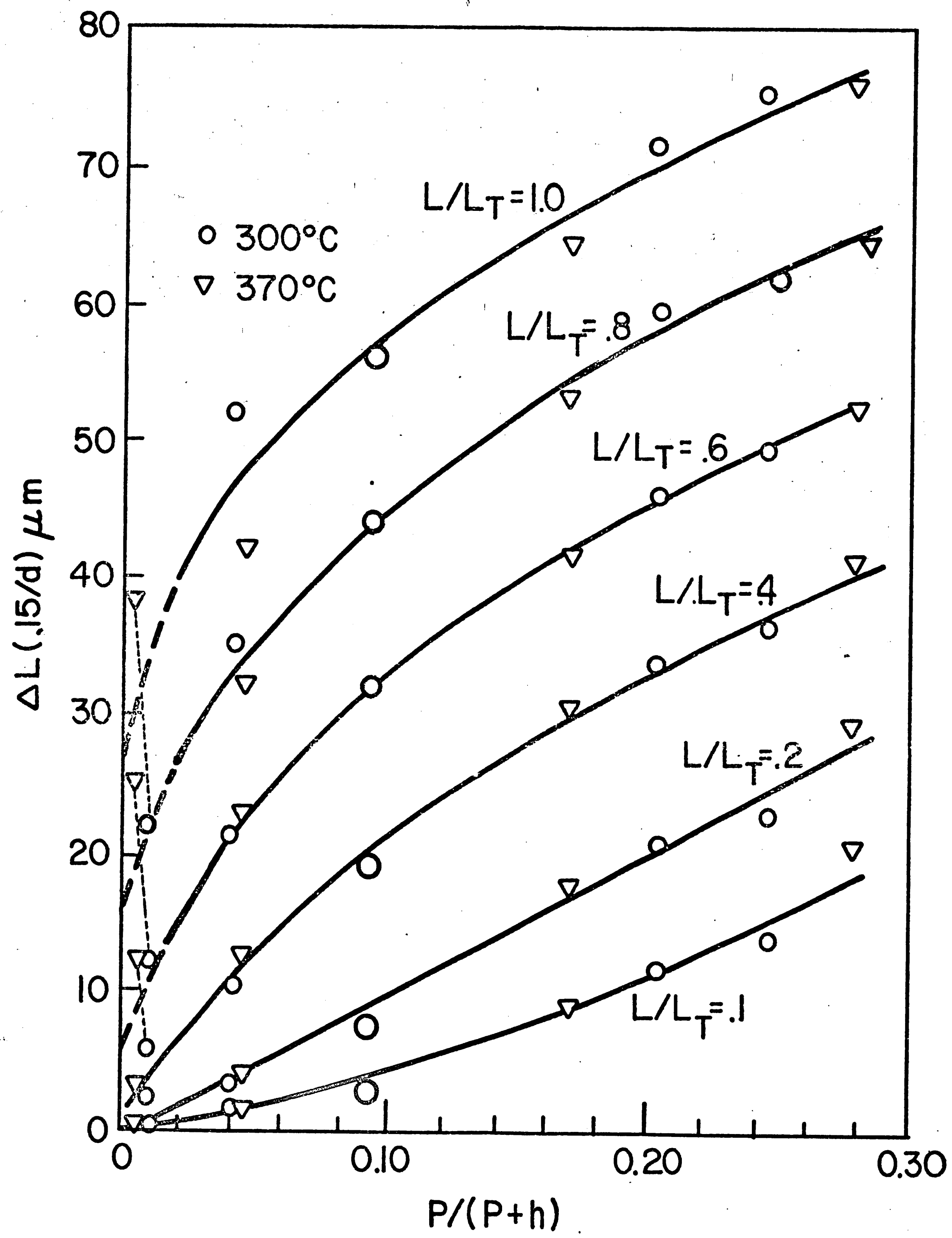


FIG. 14. NORMALIZED MARKER MOTION VS. $P_I/(P+H)_I$ RATIOS.

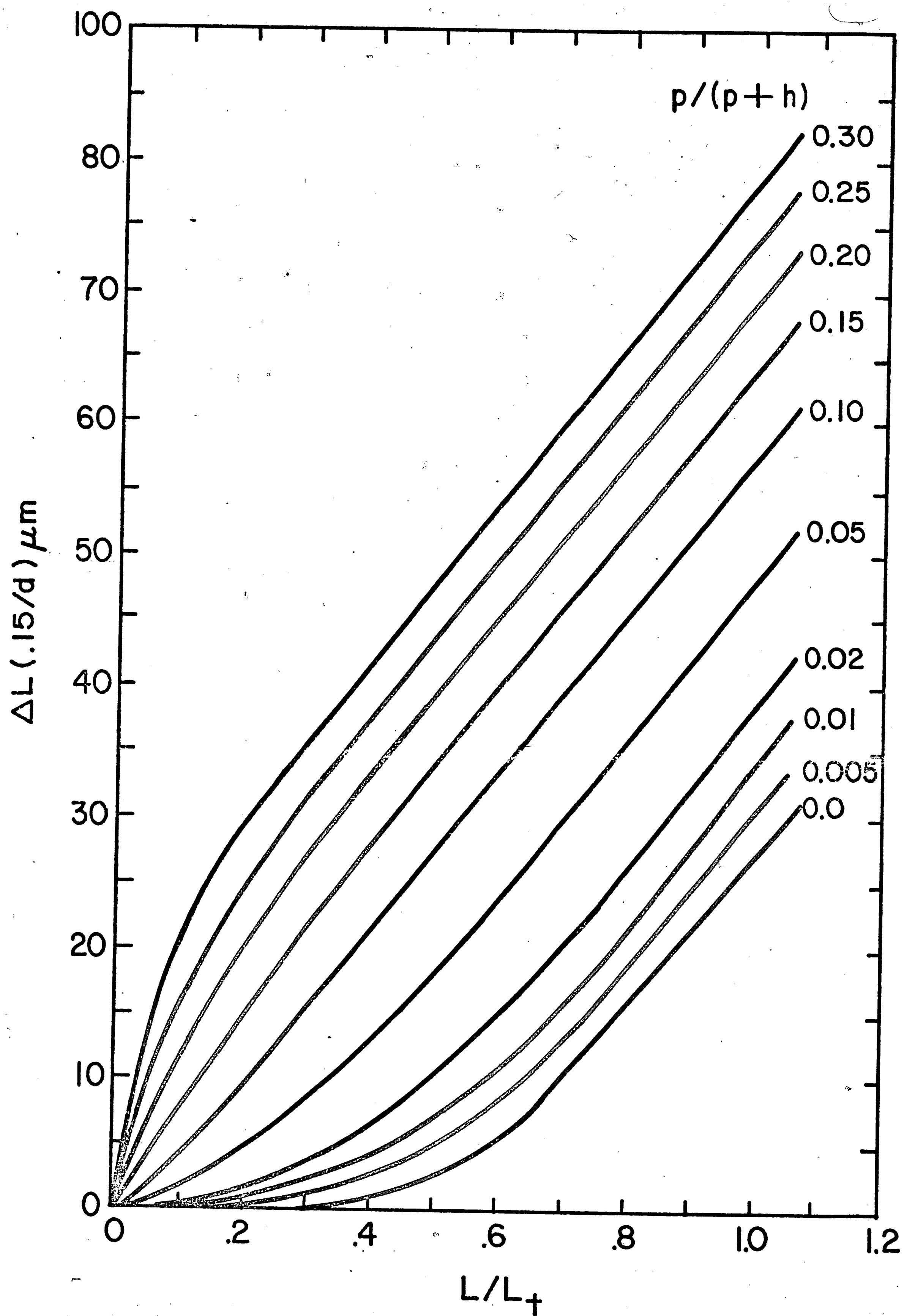


FIG. 15. NORMALIZED MARKER MOTION VS. DISTANCE FROM CENTER.

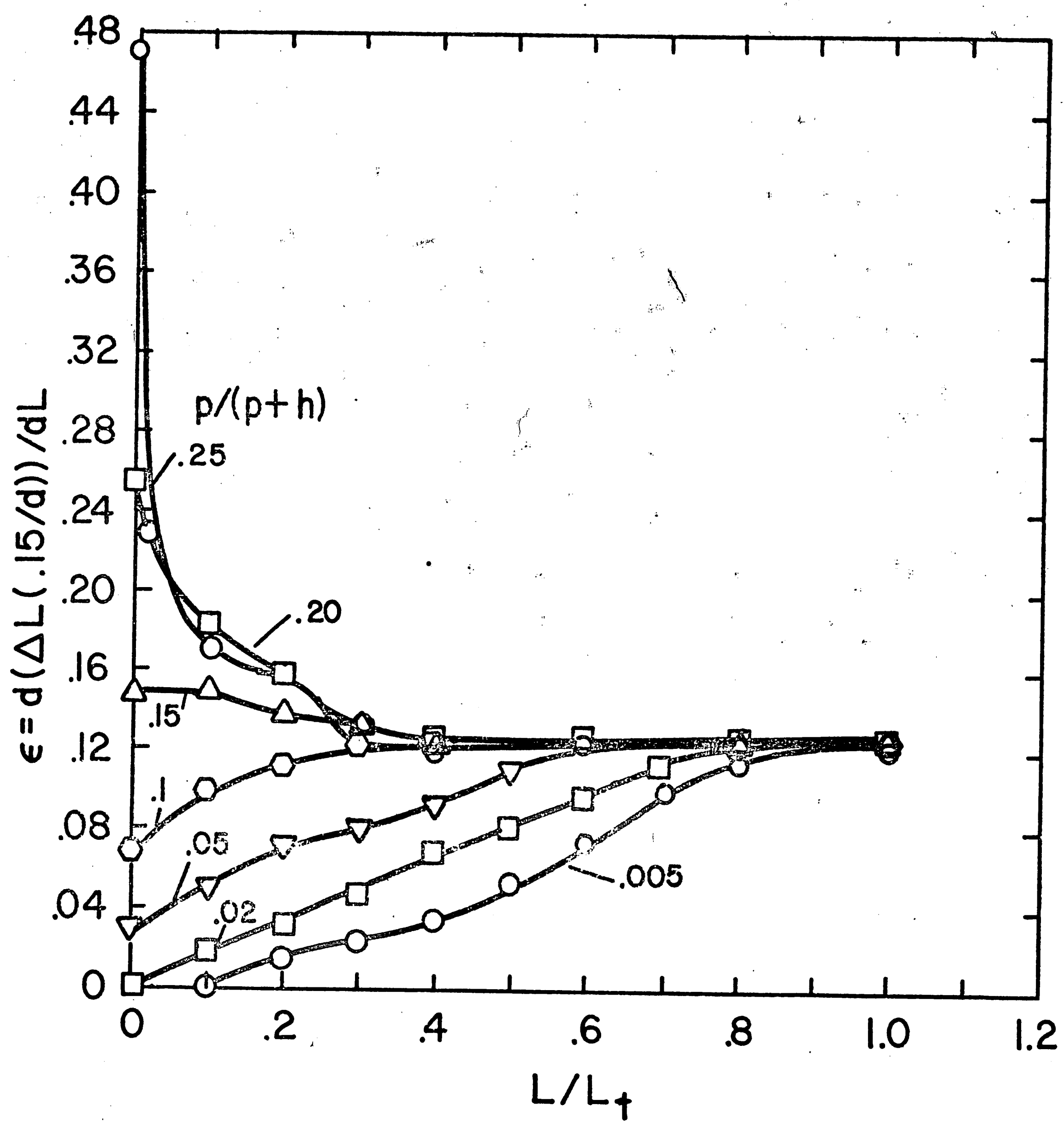


FIG. 16. TAPE SURFACE STRAINS VS. DISTANCE FROM CENTER.

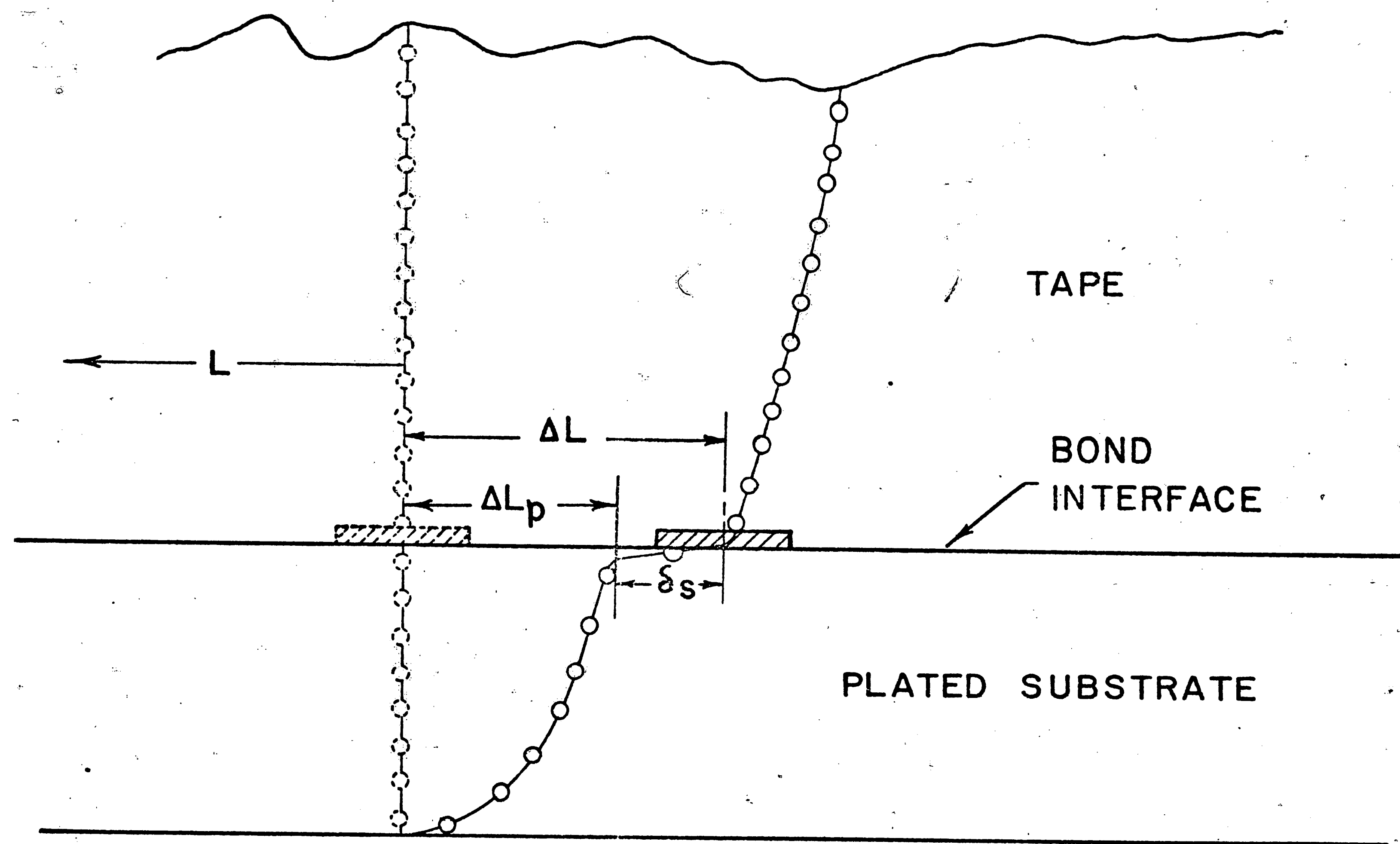
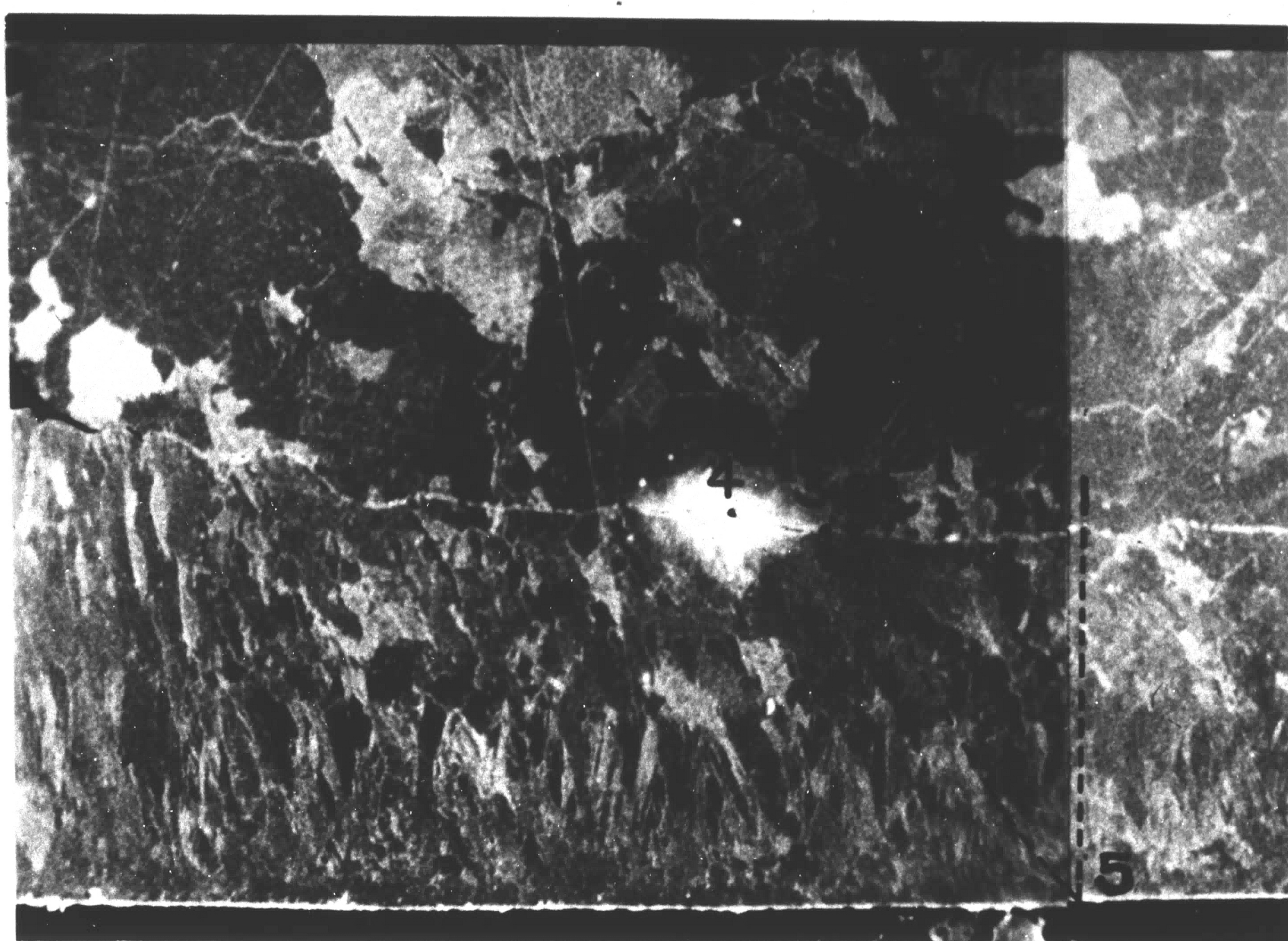


FIG. 17. SCHEMATIC DRAWING ILLUSTRATING DEFINITION OF SURFACE SLIDING, δ_s .



H-3259-A

FIG. 18. PHOTOMICROGRAPH OF INTERFACE SHOWING
PROPOSED ΔL_p AND δ_s .



H-3259

FIG. 19. PHOTOMICROGRAPH OF INTERFACE SHOWING
PROPOSED ΔL_p AND δ_s .

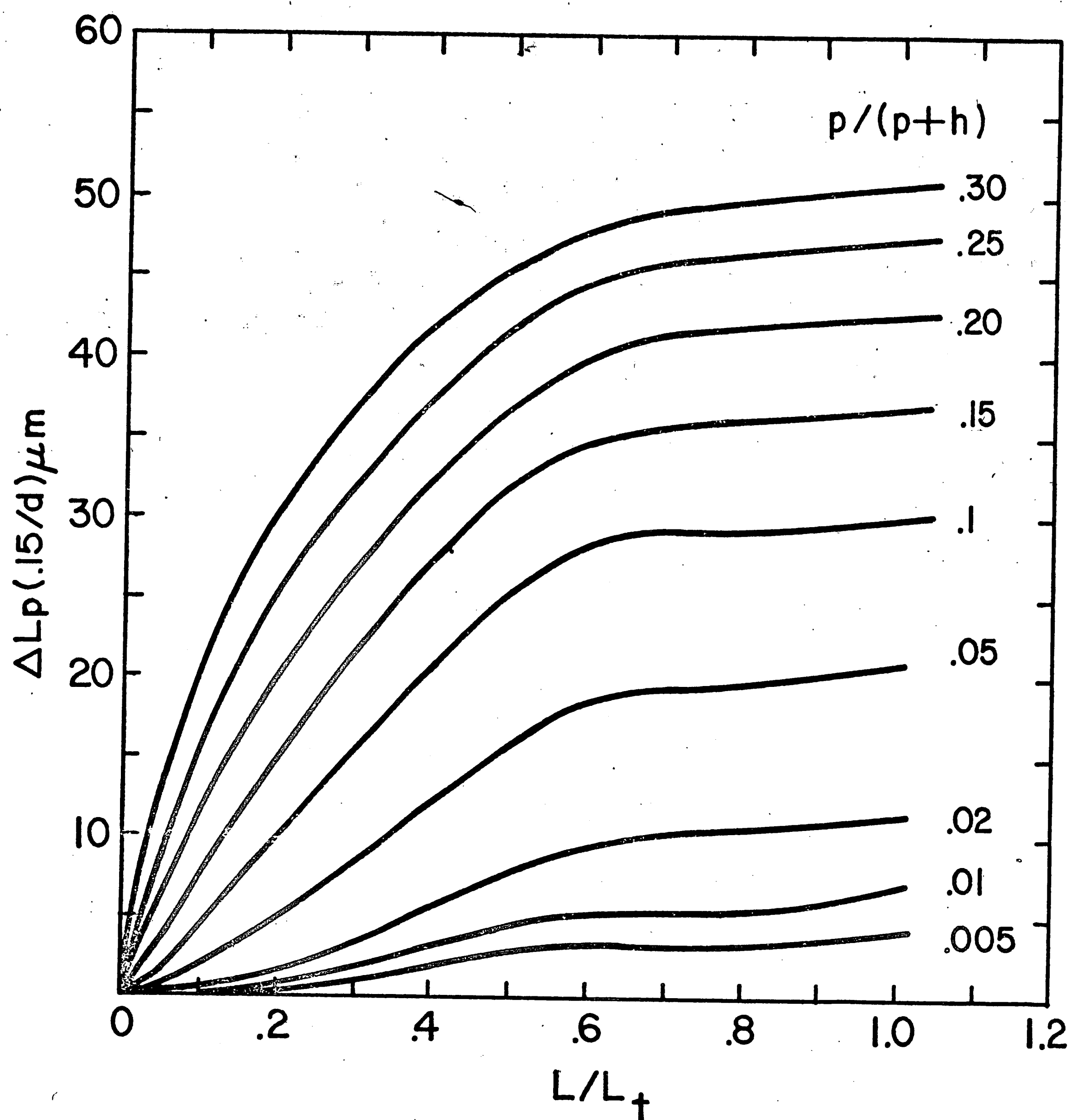


FIG. 20. NORMALIZED SURFACE MOTION OF SUBSTRATE PLATING VS. DISTANCE FROM CENTER.

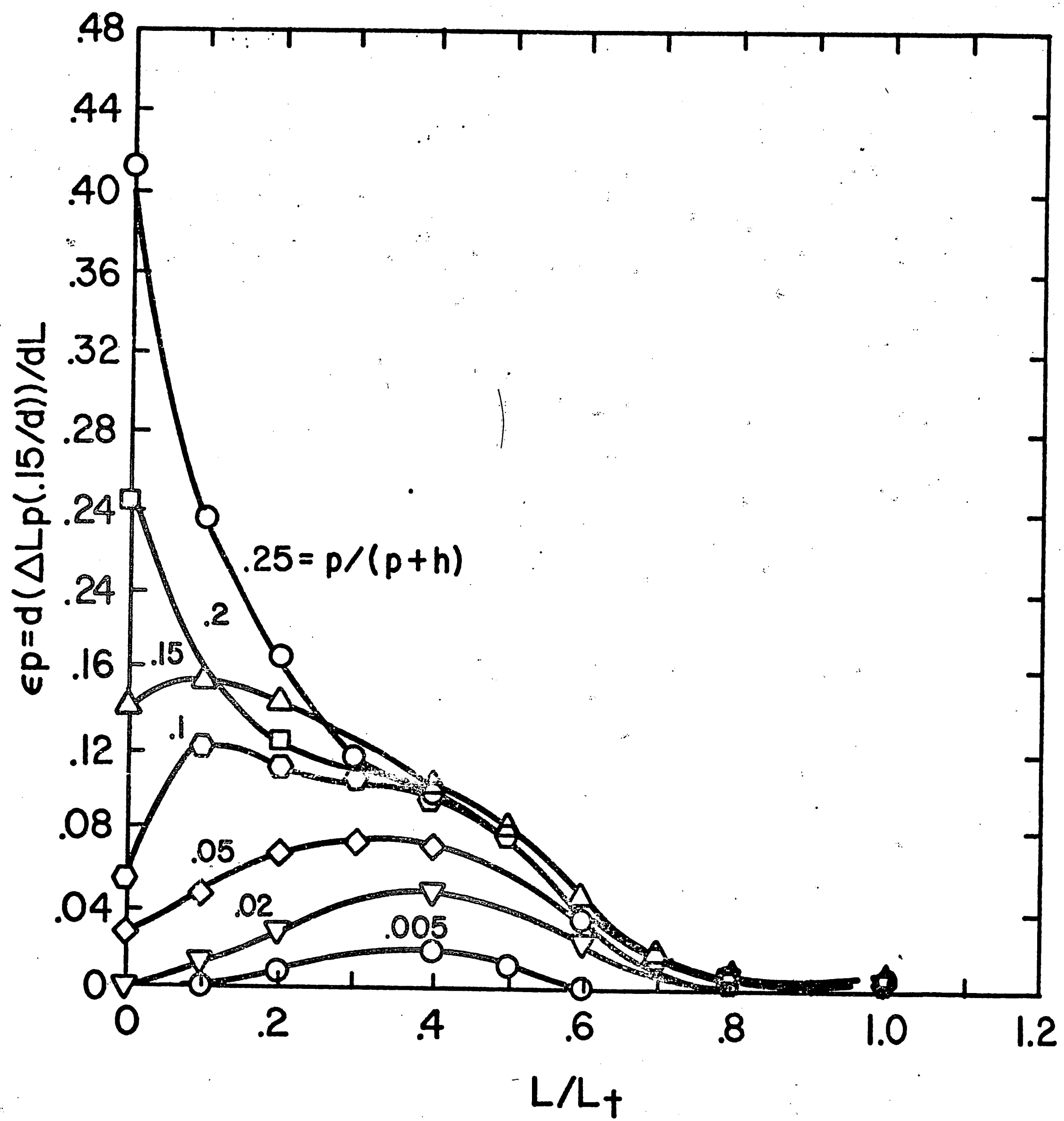


FIG. 21. SUBSTRATE PLATING STRAINS VS. DISTANCE FROM CENTER.

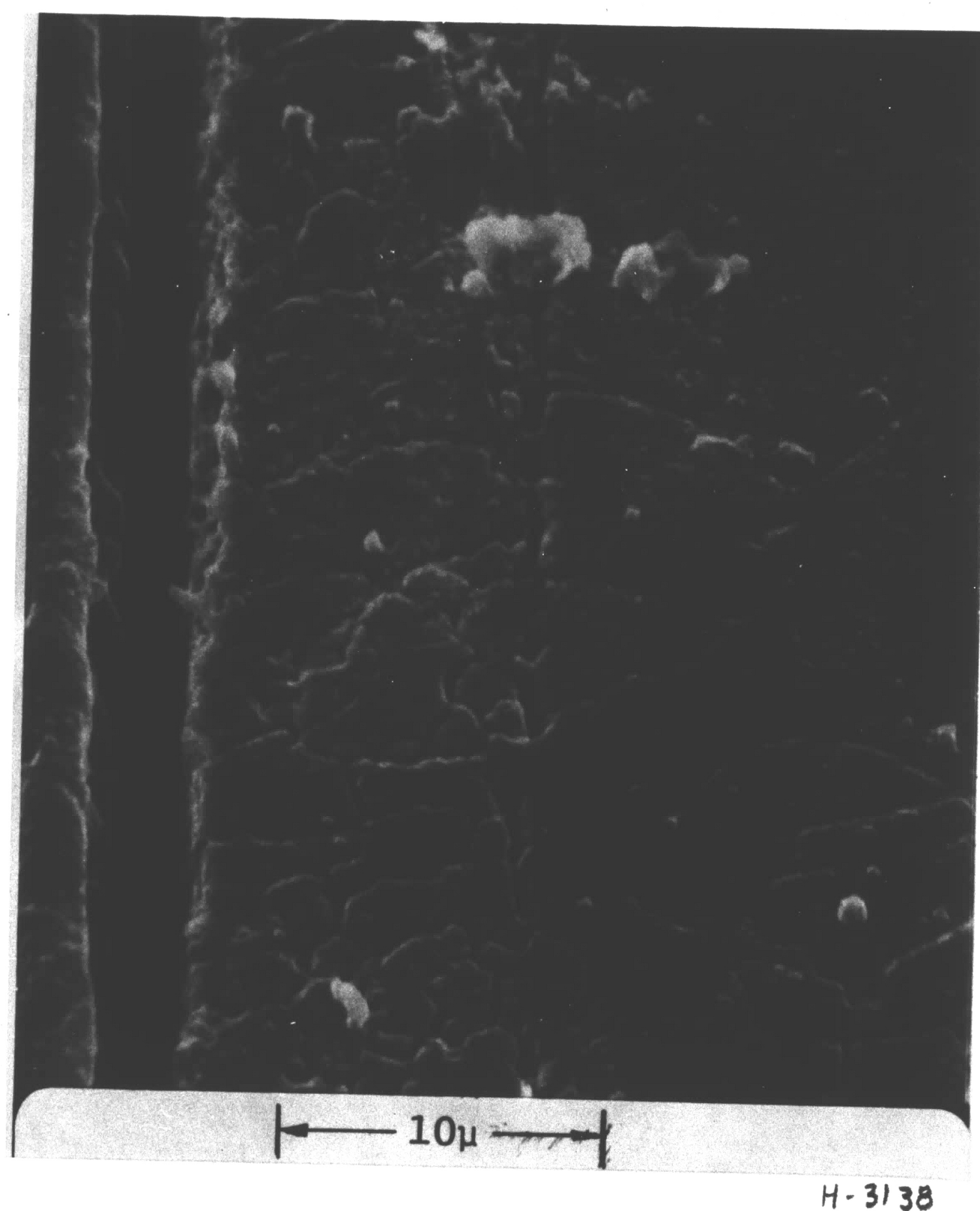
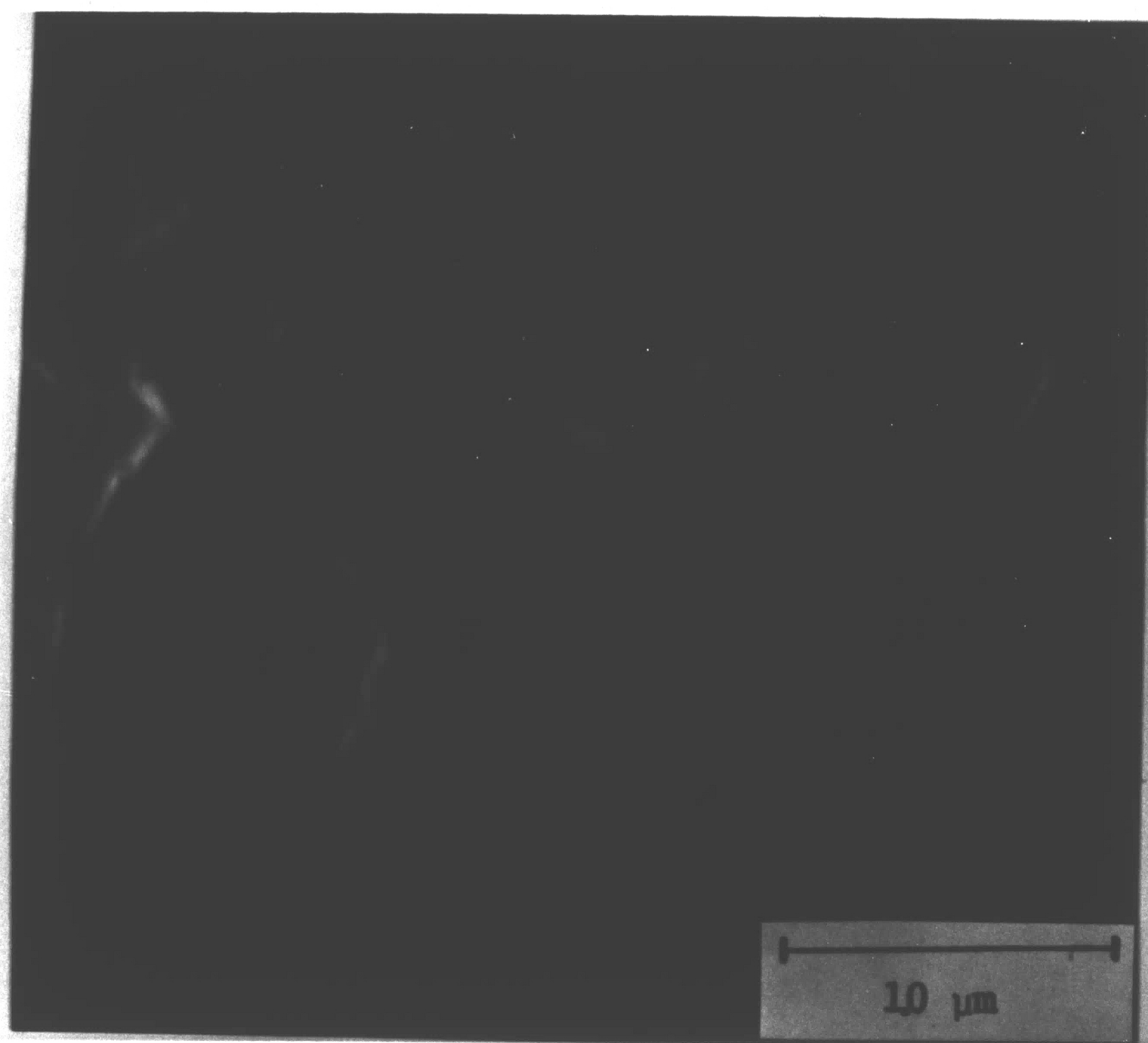


FIG. 22. SCANNING ELECTRON PHOTOMICROGRAPH OF
GRAIN BOUNDARY SWEEP BOND INTERFACE.
300X.



H-3246

FIG. 23. SCANNING ELECTRON PHOTOMICROGRAPH
SHOWING A TWIN CROSSING THE INTERFACE.
10,000X.



H-3246-A

FIG. 24. SCANNING ELECTRON PHOTOMICROGRAPH OF
FIG. 23. AT HIGHER MAGNIFICATION.
30,000X.

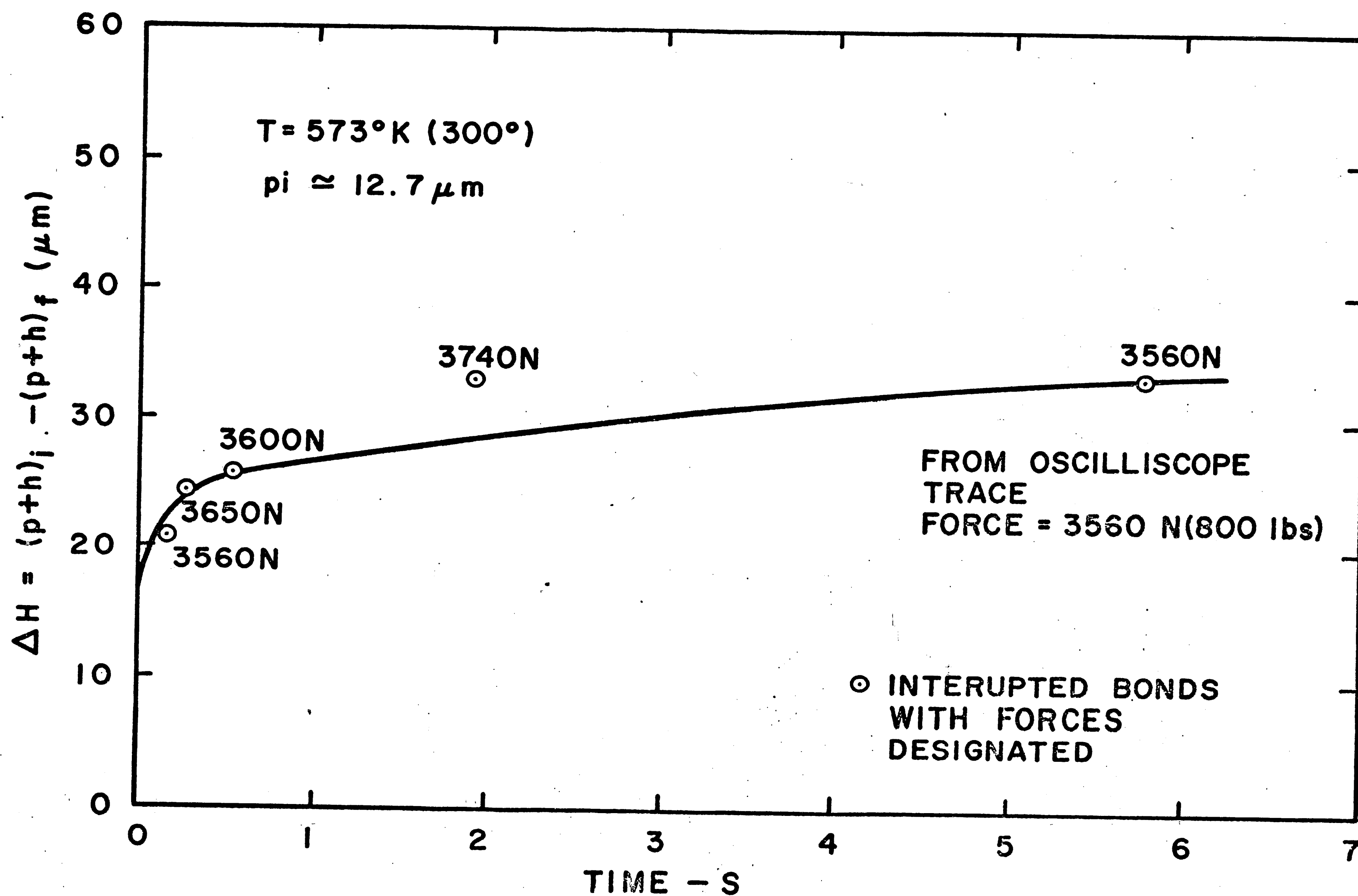


FIG. 25. RECONSTRUCTED REDUCTION IN HEIGHT VS. TIME CURVE.

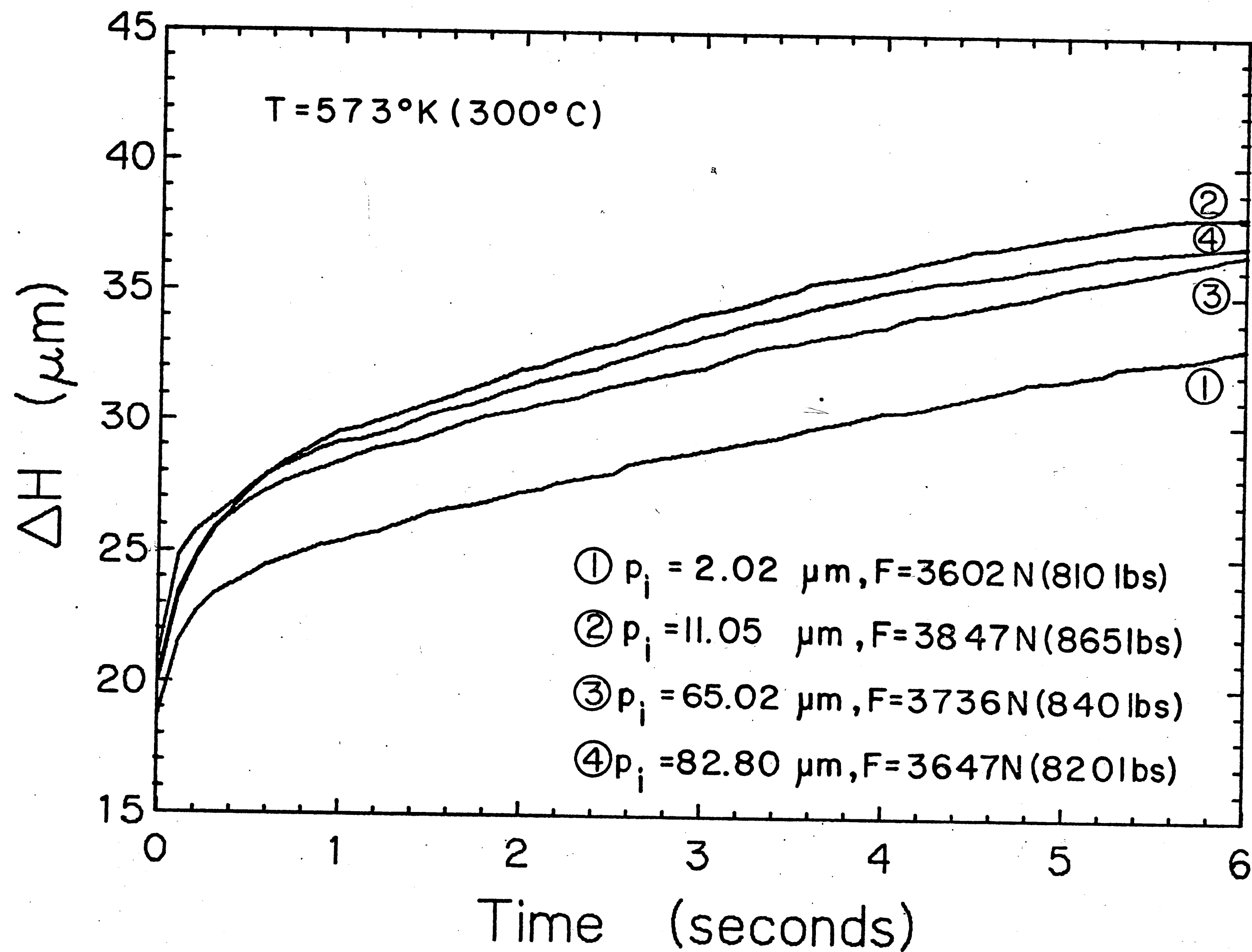


FIG. 26. REDUCTION IN HEIGHT VS. TIME CURVES FOR SAMPLES DEFORMED AT $573^{\circ}\text{K} (300^{\circ}\text{C})$.

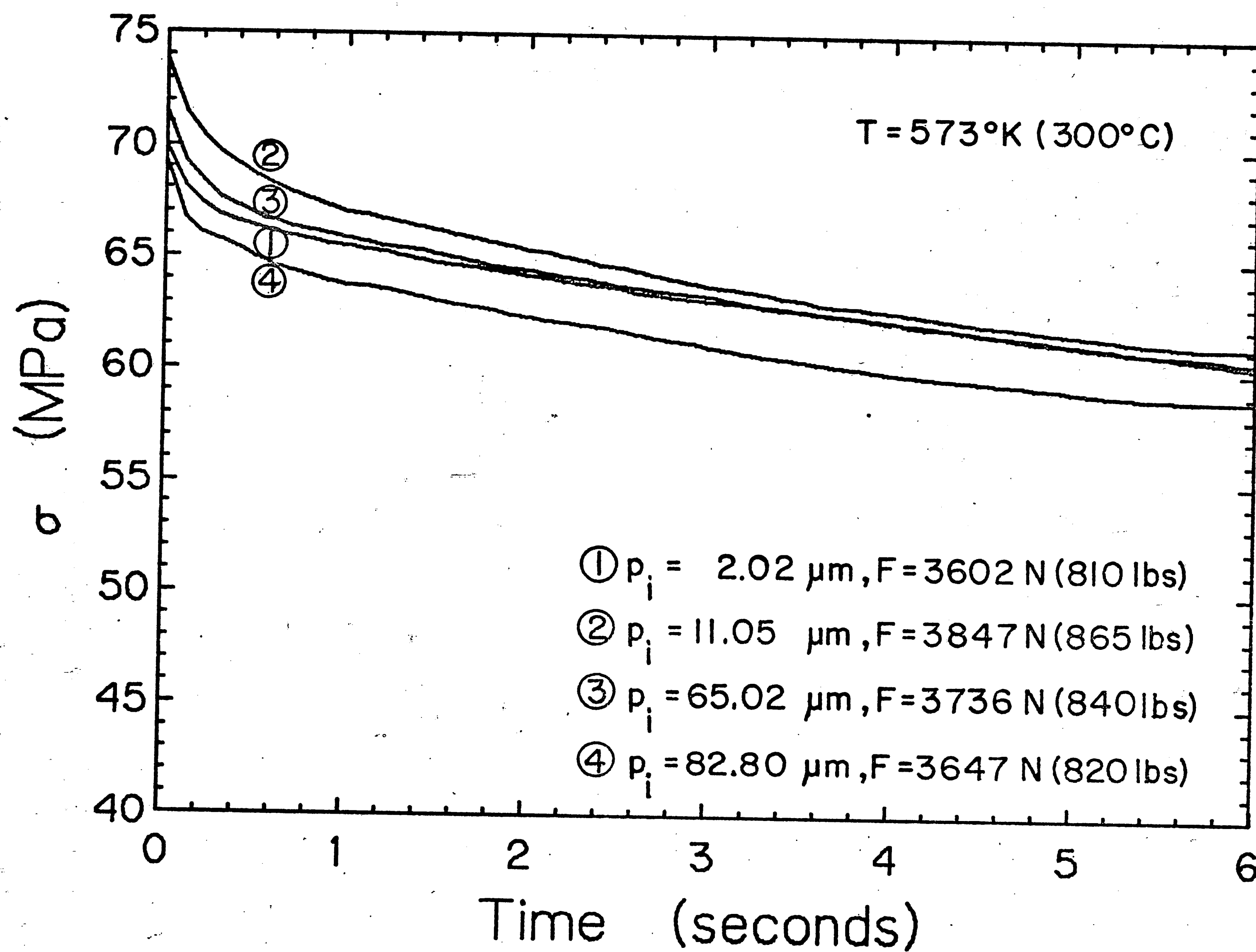


FIG. 27. INSTANTANEOUS FLOW STRESS, σ_0 , FOR SPECIMENS DEFORMED AT $573^{\circ}\text{K} (300^{\circ}\text{C})$.

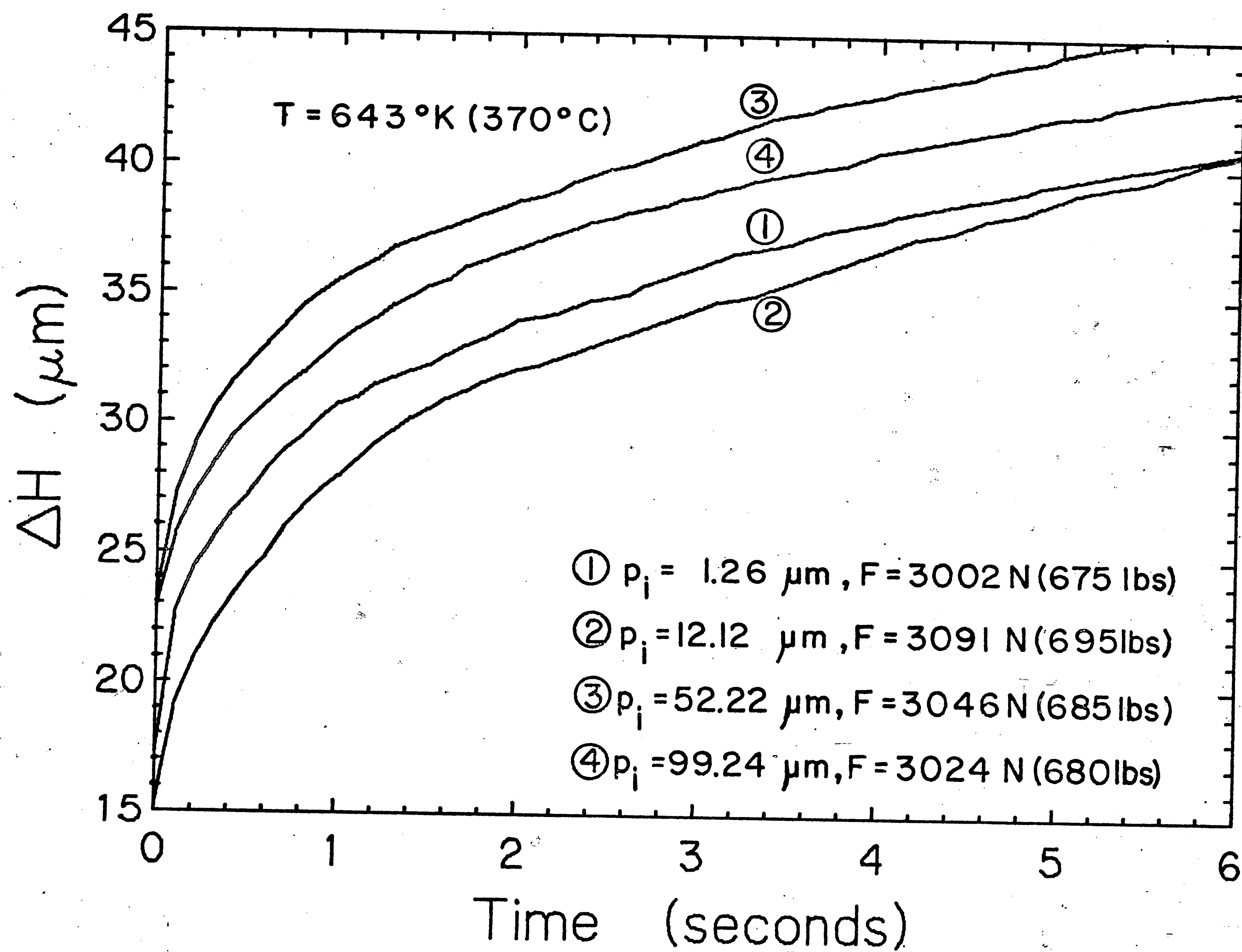


FIG. 28. REDUCTION IN HEIGHT VS. TIME CURVES FOR SAMPLES DEFORMED AT $643^{\circ}\text{K} (370^{\circ}\text{C})$.

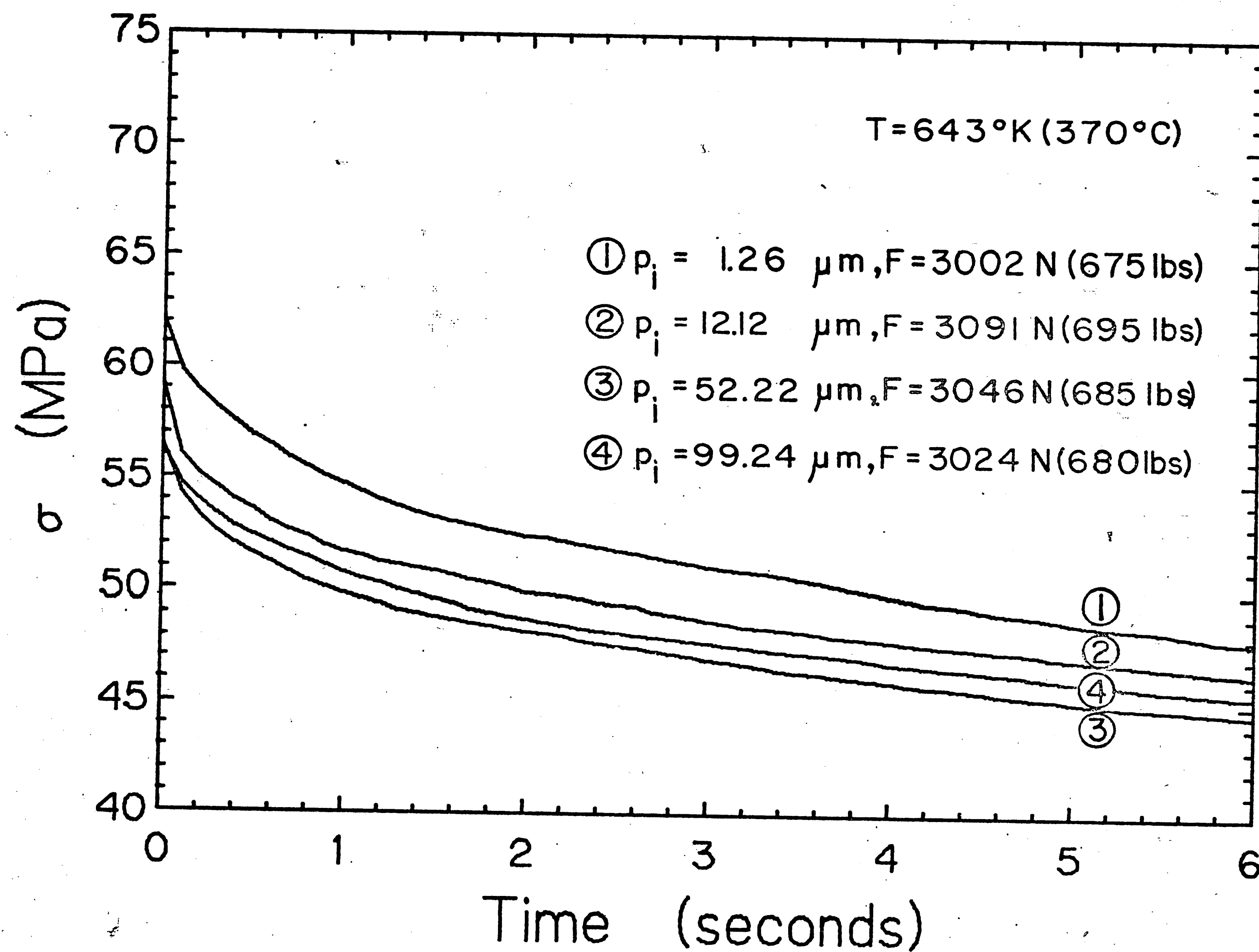


FIG. 29. INSTANTANEOUS FLOW STRESS, σ_0 , FOR SPECIMENS DEFORMED AT $643^{\circ}\text{K} (370^{\circ}\text{C})$.

BIBLIOGRAPHY

1. Johnson, K. I., "Thermal Compression and Ultrasonic Microbonding Techniques," Ultrasonics, 6, (1968), pp. 14-18.
2. Anderson, O. L., Christensen, H., and Andreatch, P., "Technique for Connecting Electrical Leads to Semiconductors," J. Applied Physics, 28, August (1957), p. 923.
3. McCann, C. D., and Reid, B. K., "Assembly of Beam Leaded Devices," Industrial and Scientific Conference Management, June (1971).
4. Clark, J. E., "The Case for Beam Lead Bonding," Electronic Packaging and Production, October (1970).
5. Coucoulas, A., "Compliant Bonding," Proceedings Electronic Components Conference, (1970), pp. 380-389.
6. Deutsch, R. J., "Assembly and Bonding of Thin Film Hybrid Circuits," Western Electric Engineer, January (1969), p. 2.
7. Adams, J. R. and Bonham, H. B., "Analysis and Development of a Thermocompression Bond Schedule for Beam Lead Devices," Proceedings Electronic Components Conference, (1972), pp. 325-331.
8. Anderson, O. L., "The Role of Surface Shear Strains in the Adhesion of Metals. Part I," Wear, 3, (1960), pp. 253-273.
9. Ellington, T. S., "Lead Frame Bonding," Proceedings Electronic Components Conference, (1972), pp. 357-359.
10. Proposed "Thermocompression Bonding of Gold Beam Lead Standard," Society of Automotive Engineers, G-8 Subcommittee on Beam Lead Bonding.
11. Milner, D. R. and Rowe, G. W., "Fundamentals of Solid Phase Welding," Metallurgical Reviews, 7, No. 12, (1962), pp. 433-480.
12. Tylecote, R. F., The Solid Phase Welding of Metals, St. Martins Press, New York, 1968.
13. Agers, B. M. and Singer, A. R. E., "The Mechanism of Small Tool Pressure Welding," British Welding Journal, 11, (1964), pp. 313-319.
14. Joshi, K. C., "The Formation of Ultrasonic Bonds Between Metals," Welding Journal, 50, No. 12, December (1971), pp. 840-848.

15. Avitzur, B., Metal Forming: Processes and Analysis, New York: McGraw-Hill, (1968), pp. 359-397.
16. Condra, L.W., "The Flow Stress of Polycrystalline Gold in Plane Strain Compression," Master's Thesis, Metallurgy and Materials Science, Lehigh University, Bethlehem, Pa., (1972).

APPENDIX A

Gold Plating for Substrate Generation

A phosphate type gold plating bath was used to generate all experimental substrate samples. This bath was chosen because of its high purity of deposit, bath efficiencies, and plating rates. Using a direct current power supply, the bath produced smooth level surfaces for the metallization samples, but as the plating thicknesses were increased above .051 mm (.002 in) a nodular surface was obtained. The bath has the following composition and operating characteristics:

potassium gold cyanide	20 gm/l
potassium phosphate monobasic	10 gm/l
potassium phosphate dibasic	40 gm/l
water (distilled) to makeup final volume	
current density	1-10 ma/cm ²
ph (electrometric) 6.5 or greater measured at 298°K (25°C)	
continuous agitation.	

PH adjustments to the bath were made by additions of phosphoric acid and potassium phosphate (monobasic) to lower or raise the ph to the 6.5 value. A gold anode was used whose purity was nominally 99.999%.

The substrates received a pre-plating clean just prior to plating which consisted of the following steps:

1. Immersed in boiling trichlorethylene for five minutes.
2. Soaked in warm trichlorethylene for ten minutes.

3. Rinsed with acetone
4. Rinsed with ethyl alcohol.
5. Dried with nitrogen gas.

If care was not taken to clean all of the organics from the surfaces, an impure metallization was deposited and the bath became contaminated. The samples were placed in a fixture, see Fig. 1, that gave each substrate the same plating area. The substrate was contacted by a gold flashed 0.051 mm (0.002 in.) ribbon which was used to provide electrical continuity. Upon completion of plating the samples were rinsed with water, acetone, ethyl alcohol, and dried with nitrogen gas. All samples received a post-plating bake at 323°K (50°C) for one-half hour. By following the cleaning procedures and giving the samples the bake, there was good adhesion between the plated gold and the stainless steel substrate which did not degrade when bonded. Elimination of the 323°K (50°C) bake or substitution of a dilute HCl etch for the pre-plating clean resulted in poor adhesion.

APPENDIX B

Marker Generation

Markers were generated on specimen tapes using a photolithic process similar to those in use throughout the semiconductor and thin film industry. The process involves the deposition of a uniform layer of photosensitive material (photoresist), exposing the photoresist to a light source through a pattern generation mask, removing the undesired photoresist with an appropriate developer, and etching the desired pattern into the material using an acid etchant. There are many choices of commercially available photoresists and selection of a particular type depends on its ultimate use.

A positive type photoresist, Shipley AZ1350H, was selected for this marker generation process. AZ1350H was chosen because it has good surface adhesion, low pin hole count, low edge build-up, a thickness of 3 μm (when applied at 5000 rpm), good pattern definition, compatibility with both the etching of gold and the plating of silver used to generate markers.

A pre-photoresist clean was given to the tapes and consisted of rinsing in acetone, then in alcohol, dried with nitrogen gas, and baked at 323°K (50°C) for one-half hour. The best surface adhesion was obtained when the tapes were cleaned just prior to application of the photoresist.

To obtain a uniform photoresist thickness, a Plat Engineering Co. spinner was used to spin the samples. This spinner has a fast

rise time which aids in reducing the photoresist edge build-up and a vacuum chuck to hold the samples. All samples were spun at 5000 rpm for ten seconds. Just before initiation of the spin cycle, the surface of the samples was completely covered with photoresist. Application of the photoresist while spinning the samples results in a non-uniform layer on the sample and difference in layer depth from sample to sample. All samples were then given a drying bake at 323°K (50°C) for one-half hour.

A 200 watt high pressure mercury arc lamp and condenser was used to expose the samples through a mask with 0.0254 mm (0.001 in.) lines on 0.3048 mm (0.012 in.) centers for two minutes. The samples were developed for two minutes in a Shipley AZ developer mixed 1:1 with water and then rinsed thoroughly with de-ionized water. The above water-developer proportions allow a continuation of the developing cycle after the water rinse to remove additional photoresist. A post-develop bake at 323°K (50°C) for one-half hour was given to all samples to insure good surface adhesion.

To etch the markers into the gold samples, a saturated solution of KI and I_2 was used with a composition as follows:

800 gm. KI

450 gm. I_2

700 ml. H_2O .

This etchant etches at a 2 - 3 μ m/min rate. The total etch time for the 4 μ m deep grooves was one and one-half minutes.

During the use of the process, it was observed that:

1. Thorough pre-photoresist cleaning is important to surface adhesion.
2. All baking steps must be used to avoid creep of the etchant between the photoresist and the gold surface.
3. Care should be taken to shield the samples from room light to avoid degradation of the photoresist.
4. The photoresist must be applied prior to spin cycle to avoid a non-uniform layer of photoresist on the sample.

APPENDIX C

Silver Plating Solution and Procedures

The selection of silver as a marker media provided a FCC metal having properties similar to gold but can easily be seen when plated in the gold tapes. Although silver will oxidize, the amount of tape surface affected is less than 8 percent. The markers were plated through the same photoresist window used for etching grooves in the tapes as described in Appendix B. To avoid degradation of the photoresist, the silver plating solution must have an operating electrochemical pH of less than 8.

The original bath selected had the following composition and operating characteristics:

Silver Nitrate	20 g/l
Ammonium Hydroxide	50 ml/l
Ammonium Sulfate	120-200 g/l
Temperature	291°K-318°K (18°C - 45°C)
Current Density	.8 amps/cm ²
pH (electrochemical)	6.6-6.9

Due possibly to the small exposed surface area, it was found difficult to control the current density well enough to avoid modular deposits. The following slightly modified bath gave smooth deposits and good adhesion.

Silver Nitrate	20 g/l
Ammonium Hydroxide	25 ml/l
Ammonium Sulfate	200 g/l

Temperature 335°K (62°C)

pH (electrochemical) 6.6-6.9

No external emf is applied when plating markers with this bath. A copper "alligator" clip was clamped to one end of the tape and partially immersed in the electrolyte. This setup on an emf cell and also regulated the current. Plating results from the fact that the gold has a higher electronegativity than copper and silver is lower than either the copper or gold.

Using this procedure, the tapes were plated up to the top of the etched grooves with a fine grained silver. The total plating time was four seconds. To insure good surface adhesion of the silver, the tapes were etched for five seconds in a KI and I₂ solution just prior to plating and rinsed thoroughly with de-ionized water.

The plating rate of the bath can be reduced if the operating temperature is lowered. However, operating the bath at lowered temperatures produced more nodular surface topography and the adhesion to the gold surface was poor.

APPENDIX D

A Pure Gold Polishing Technique

The following technique is a generalization of the polishing procedure that was used to prepare the samples of this investigation. Each sample showed some peculiarity during the polishing however none were unique enough to be reported here.

During the initial grinding of soft metals, material beneath the surface is disturbed by occasional scratching. As additional material is removed, these scratches are covered and are not visible. However, these scratches will reappear when the metal is etched. It is, therefore, essential that the worked layer of metal be removed by means other than mechanical prior to continuation of the polishing procedure. It is conventional to etch the worked layer between polishing steps. The etchant used for this was a modified aqua regia and consisted of a solution of five parts HCL and three parts HNO_3 . The etch rate appeared to be consistent from between 20 minutes to four hours after preparation of the etchant.

After conventional grinding of the surface down to five μm , the samples were etched in the modified aqua regia for 10 seconds at room temperature. The final polishing procedure utilized 5 μm , 1 μm , and .05 μm alumina slurry in successive steps.

A nylon cloth was used for the 5 μm alumina polish while a shaved high-nap microcloth was used for the remaining two steps. An additional .05 μm alumina polish and a 6 second etch was given

each sample. All etching was done by swabbing. The samples were thoroughly rinsed with de-ionized water and dried with nitrogen gas. This latter step was necessary to prevent the continuation of etching during sample storage.

VITA

Leon Dries, the son of Mr. and Mrs Edward J. Dries, was born in Bowdle, South Dakota, on September 7, 1938. He graduated from the Cathedral of the Immaculate Conception High School in Rapid City, South Dakota in June of 1956 and received his Bachelor of Science degree in Electrical Engineering from South Dakota School of Mines and Technology in June of 1966. From 1966 to 1968, he was employed by Western Electric Company at the Bell Telephone Laboratories in Whippany, New Jersey, where he was involved in the design of thin film microwave circuits. In September 1968, he was assigned to Western Electric's Allentown Works in Allentown, Pennsylvania, where he performed failure mode analysis on beam leaded, silicon integrated circuits. Since June of 1971, he has been assigned to Western Electric's Corporate Education Center in Princeton, New Jersey, as a member of the Lehigh Masters Class of 1973.